Preliminary Study of Infrasonic Attenuation and Dispersion in the Lower Thermosphere
Based on Non-continuum Fluid Mechanics: Developing a Predictive Model

A Thesis

Presented to the

Graduate Faculty of the

University of Louisiana at Lafayette

In Partial Fulfillment of the

Requirements for the Degree

Master of Science

Akinjide Akintunde

Spring 2014

Preliminary Study of Infrasonic Attenuation and Dispersion in the Lower Thermosphere
Based on Non-continuum Fluid Mechanics: Developing a Predictive Model

Akinjide Akintunde

APPROVED:

_____   _____
Andi Petculescu, Chair   Gabriela Petculescu
Assistant Professor of Physics   Associate Professor of Physics

_____   _____
James Dent   Mary Farmer-Kaiser
Assistant Professor of Physics   Interim Dean of the Graduate School

Acknowledgments

Table of Contents

List of Figures

Abbreviations and Symbols

A^T	Transpose of matrix A
$\vec{B} = \vec{B}_0 + \vec{B}_1$	Total magnetic field strength ($Tesla$)
c_p, c_v	Specific heat capacities at constant pressure and volume respectively ($Jkg^{-1}K^{-1}$)
e_α	Species charge (C)
f	Sound frequency (Hz)
$\vec{K} = {\omega}/{c(\omega)} + i \propto (\omega)$	Wave number (m^{-1})
$Kn = {L}/{\lambda}$	Knudsen number
L	Mean free path (m)
MHD	Magnetohydrodynamics
M	Molar mass of air ($kgmol^{-1}$)
m_α	Species mass (kg)
n_α	Species number density (m^{-3})
NASA	National Aeronautics and Space Administration
NIST	National Institutes of Standards and Technology
NOAA	National Oceanic and Atmospheric Administration
$p = p_0 + p_1$	Total pressure (Pa)= ambient + fluctuation
R	Universal gas constant (8.314 $Jmol^{-1}K^{-1}$)
$T = T_0 + T_1$	Total Temperature (K)

U	Internal energy (J)
USAF	United States Air Force
$\vec{v} = \vec{v}_0 + \vec{v}_1$	Particle velocity = wind velocity + fluctuation
$\vec{v}_A = \vec{B}_0 \big/ \sqrt{\mu_0 \rho_0}$	Alfvén wave velocity (ms^{-1})
$\vec{v}_\alpha$	Average or drift velocity of species
$\omega = 2\pi f$	Angular frequency $(rads^{-1})$
$\propto (\omega)$	Absorption coefficient $[Npm^{-1}\ or\ dB(km)^{-1}]$
λ	Wavelength (m)
∂_t	Explicit time derivative
$D_t = \partial_t + \vec{v} \cdot \nabla$	Convective derivative
$\rho_1, p_1, \vec{v}_1, T_1 = \lvert \rho_1, p_1, \vec{v}_1, T_1 \rvert e^{i(\vec{K}\cdot\vec{r} - \omega t)}$	Fluctuations due to sound propagation
$\rho = \rho_0 + \rho_1$	Total mass density (kgm^{-3}) = ambient + fluctuation
η	Shear viscosity $(Pa.s)$
$\overleftrightarrow{\sigma} = p\overleftrightarrow{I} + \overleftrightarrow{\sigma}'$	Stress tensor
$\overleftrightarrow{I}$	Identity tensor
$\overleftrightarrow{\sigma}'$	Viscous stress tensor
μ	Dynamic viscosity $(Pa.s)$
λ_μ	Second coefficient of viscosity $(Pa.s)$

$$\xi = \lambda_\mu + {}^2\!/_3\, \mu$$

Bulk viscosity $(Pa.\,s)$

$$\eta = \xi + {}^4\!/_3\, \mu$$

Total viscosity $(Pa.\,s)$

$$\epsilon_1 = 1.017, \epsilon_2 = 0.8 \text{ and } \epsilon_3 = 1.014$$

Intermolecular force constants for elastic spheres (Mason, 1965)

$$\beta_T = {}^1\!/_{\rho_0} \left({}^{\partial\rho}\!/_{\partial p} \right)_T$$

Isothermal compressibility (Pa^{-1})

$$\propto_p = -{}^1\!/_{\rho_0} \left({}^{\partial\rho}\!/_{\partial T} \right)_p$$

Isobaric coefficient of thermal expansion (K^{-1})

$$\mu_0$$

Magnetic permeability of air (NA^{-2})

Chapter 1: Introduction

1.1 Infrasound: Background and Facts

Infrasound is the region of the acoustic spectrum covering frequencies < 20 Hz, which is the lower limit of the audible range. Infrasonic waves are generated by natural phenomena such as auroras, avalanches, earthquakes, meteors and volcanoes, large animals, machinery (e.g. wind turbines and high-bypass jet engines), as well as nuclear and conventional explosions. These low-frequency compression waves were first observed on a global scale after the eruption of the Krakatoa volcano, Indonesia, in 1883. Infrasound records have been attributed to events such as Oppau explosion, Germany in 1921, Buncefield oil depot explosion, United Kingdom 2005, Chelyabinsk meteor, Russia in 2013 and nuclear tests by North Korea in 2013. Compared to audible sounds, infrasound energy losses are much smaller owing to their low frequencies. Hence, an infrasonic signal can propagate over large distances, reaching altitudes of more than 100 km (Blanc and Ceranna, 2009). That is why infrasound can be used in atmospheric studies, prediction of natural disasters, and in detecting tests of chemical and nuclear ordnance. The Comprehensive Nuclear-Test-Ban Treaty Organization (CTBTO) was established in 1997 to monitor clandestine nuclear explosions. This is done through a continuously growing network of infrasound detector arrays. Presently, the network consists of 60 infrasound stations of 337 monitoring facilities, complemented by the seismic, hydro-acoustic, and radionuclide stations of the International Monitoring System (IMS).

1.2 Atmospheric Propagation of Infrasound

The long-range propagation of infrasound in the atmosphere is affected by the vertical sound speed profile. Sound speed varies as the square root of temperature and is also subject to the

effects of the winds. Under typical conditions, starting at sea level, the speed of sound decreases due to decreasing ambient temperature. In the upper stratosphere, absorption of solar UV radiation by ozone causes a positive temperature gradient, up to about 45 km. Above this height, the temperature decreases again through the mesosphere. In the thermosphere, solar X-rays and extreme-UV (XUV) radiation at wavelengths < 170 nm are almost completely absorbed, resulting in a steep positive temperature gradient. Also in the thermosphere, the energetic radiation causes dissociation and ionization of air molecules, leading to the ionospheric layers. Principal propagation channels are the stratospheric duct, formed between the ground and the stratopause and the thermospheric duct, formed between the ground and about 100 km in the thermosphere. Since the ducts that are formed are not rigid, sound leaks out of the duct back to the ground and sound propagating from the ground can be diverted back to the surface by the duct boundaries. Arrivals of infrasound from the thermosphere have been well documented in literature. An example of such measurements is shown in Figure 1.
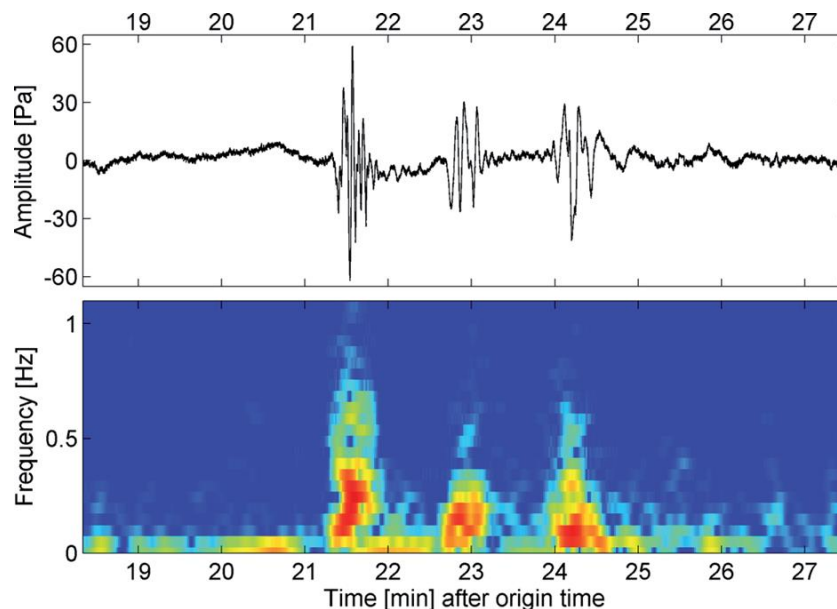
Figure 1: Top: Infrasound signal recorded in French Polynesia on Hao 450 km North-West from the source of a nuclear explosion with a yield of a few kilotons. Below: Time-frequency analysis (Blanc and Ceranna, 2009)

Typically, sounds of frequencies above 1 Hz are strongly attenuated over long atmospheric paths. The classical absorption coefficient varies as the square of frequency and inversely with pressure: therefore, frequency components of a few tenths of Hertz can propagate over long distances. This is consistent with data such as that shown in Figure 1.

1.2.1 Existing Infrasonic Attenuation Predictive Models

Sound wave travelling through air (free of fog, moist and dust) is attenuated due to atmospheric absorption caused by classical and non-classical losses (Sutherland and Daigle, 1998). The classical losses are associated with heat conduction, viscosity, and diffusion. Non-classical (or molecular) losses are associated with the relaxation of the vibrational and rotational degree of freedom of polyatomic molecules.

1.2.1.1 The Sutherland and Bass (SB) Model

The model (Sutherland and Bass, 2004) estimates atmospheric sound absorption up to 160 km. It is based on Navier-Stokes equations and linear propagation. The model sought to improve on the existing American National Standard: 'Method for calculation of the absorption of sound by the atmosphere'. Also, the model includes losses due to rotational relaxation. Absorption estimates for altitudes above 90 km are regarded as less accurate due to uncertainty in composition of the atmosphere at such high altitudes.

1.2.1.2 The Gainville and Blanc-Benon Model

A nonlinear propagation model (Gainville and Blanc-Benon, 2010) was developed to investigate two things: (1) develop an operational 3D nonlinear ray tracing code that

computes temporal pressure signatures (waveforms) at receivers of the CTBTO. This was done by solving generalized Burgers' equation (Pierce, 1981) along each eigenray linking the source to each receiver. While accounting for nonlinear effects, viscosity absorption and molecular vibration mechanisms. (2) non-linear effects relative to linear dissipative effects were quantified by the Gol'dberg number (Pierce, 1981). In the study, nonlinear effects were observed to dominate linear absorption effects on propagation of the explosion event studied (Misty Picture experiment).

1.2.1.3 The de Groot-Hedlin Model

A computational algorithm was developed (de Groot-Hedlin, et al., 2011) to model linear infrasound propagation and compare its results to the SB model. It was observed that the SB model overestimates the attenuation coefficient when compared to observed values for thermospheric returns. The conclusion is drawn that a better understanding of infrasound absorption in the thermosphere is needed.

1.3   Motivation

The propagation of acoustic waves in the atmosphere is intimately connected to the state of atmosphere (e. g. temperature, pressure, density, winds etc.). Therefore, accurate models are required that include all the relevant physical mechanisms affecting the acoustic wavenumber, such as scattering, attenuation and dispersion which control infrasonic propagation. Problems that have been identified with infrasound propagation are discussed below.

In a study of a large bolide that burst above a dense seismic network in the US Pacific Northwest on February 19, 2008, estimates of absorption obtained from currently used attenuation models (Sutherland and Bass, 2004) predict much greater attenuation for thermospheric returns at frequencies greater than 0.1 Hz than was observed (de Groot-Hedlin, et al., 2011). Two possible reasons were suggested for this observation:

1. SB model predictions for the attenuation coefficient in the thermosphere are inaccurate,

2. thermospheric returns undergo non-linear propagation at very high altitude.

Poor understanding of infrasound propagation at thermospheric altitudes has been attributed to the rarefied nature of the thermosphere. Ambient pressure ranges from $\sim 10^{-6}$ atm at 86 km to $\sim 10^{-9}$ atm at 160 km (compare to 1 atm at sea level), while Mean free path, L, ranges from $10 \: mm \: to \: 53 \: m$ in the lower thermosphere. The transition between a continuum and non-continuum regimes can be expressed in terms of the acoustic Knudsen number defined as the ratio between the mean free path of the air molecules and the acoustic wavelength ($Kn = L/\lambda$). In the physical acoustics literature, the same ratio is often expressed via the frequency/pressure (f/p) ratio, based on the kinetic theoretical dependence of pressure on the inverse mean free path. For $Kn < 0.01$, the fluid is regarded as a continuum, hence, continuum mechanics i.e. Navier-Stokes approximation is most suited for characterizing the fluid dynamics. However, for $Kn > 0.01$, non-continuum mechanics (e.g. Burnett, super-Burnett, 13-moment approximation etc.) is considered appropriate.

The thermosphere is located within the ionosphere. Hence, it contains charged species-electrons and positive ions. It is therefore expected that these charged species should have some influence on the propagation of acoustic waves. This effect of the ionosphere on

5

infrasound propagation has not been considered in existing absorption models (Sutherland and Bass, 2004; Gainville and Blanc-Benon, 2010; de Groot Hedlin, et al., 2011). In this study, a mechanism is suggested based on the following premise: the acoustic wave front incident from the neutral upper mesosphere encounters "streams" of charged particles-electrons and ions traveling along paths defined by existing magnetic and electric fields. Consequently, there will be a collisional exchange of energy between the neutral particles and the charge carriers. This exchange affects the dynamics of the neutral-charged mixture (a partially ionized plasma or PIP): the charged "streams" are perturbed by the incident acoustic wave motion and in turn, the infrasonic wavefront will lose some coherence. The former imposes fluctuations in the electron and ion current densities, as well as electric and magnetic fields. The latter effect embodies the net loss of energy, whose "imprint" is carried, upon downward refraction at the thermospheric inversion, to the ground detector.

In this work, the non-continuum fluid mechanics is applied to the problems of absorption and dispersion of infrasound in the lower thermosphere (approximately 85 to 160 km). A hypothesis of charged species within the lower thermosphere having some effect on the absorption and dispersion of infrasound is also tested in this work by incorporating the effects of electric and magnetic forces into the predictive framework to be developed.

In this work, only sources of infrasound on (or close to the) the ground are considered in order to avoid the need to include nonlinear steepening or shocking. Examples of ground-based infrasound sources of interest are avalanches, earthquakes, explosions, and strong storms. The rationale for this choice is as follows: as the wave advances into the progressively thinner layers, the particle displacements in the wavefront may increase owing to fewer collisions to the point where shocks may appear. For surface sources, steepening and/or shocking are likely to occur and persist over a few kilometers from the source. In the

6

comparatively thicker troposphere, one can assume that the higher frequency components are fast attenuated. The assumption is made that: by the time a wave reaches the thermosphere, the acoustic pressure fluctuations are smaller than the local equilibrium pressure. Therefore, one could neglect nonlinear effects. Nevertheless, this assumption may need to be revisited in future studies, especially for extremely strong low-elevation sources (e.g. airbursts like the Chelyabinsk and Tunguska events).

1.4   Continuum and Non-continuum Mechanics

Dynamical fluid parameters such as pressure, density, velocity, and temperature are obtained by solving the flow equations describing the mass continuity, conservation of momentum and energy, combined with the equation of state. These equations must be supplemented with constitutive relations expressing the transport of stresses and heat via the stress tensor and heat flux. The flow and transport equations are obtained as approximate solutions of Boltzmann Transport Equation (BTE) developed by Ludwig Boltzmann in 1872, within the context of non-equilibrium statistical mechanics (Mason, 1965). The first approximation yields the inviscid Euler equations which are appropriate for a lossless medium and therefore of no interest in this work. The second approximation yields the Navier-Stokes equations, which can accurately predict thermo-viscous flows in continuous media. In the Navier-Stokes approximation, the viscous stress tensor and heat flux are independent. The third and fourth approximations yield the Burnett and super-Burnett equations (Mason, 1965), respectively, in which the stress tensor and heat flux are coupled.

The fundamental characteristics of acoustic wave motion-phase speed (or sound speed) and attenuation coefficient enter the real and imaginary parts of the wave number respectively. Assuming that the molecules' internal and translational degrees of freedom are in thermal equilibrium, sound propagation in air is effectively non-dispersive (frequency-independent phase speed) while the attenuation coefficient of air varies with the square of the frequency. When molecular relaxation times are finite, slight dispersion will occur. In this work, a theoretical model is developed to calculate the acoustic wavenumber in the lower thermosphere, relying on ambient data (e.g. pressure, temperature, composition, mean free paths) and thermophysical parameters (e.g. specific heat capacity, viscosity, thermal conductivity) obtained from atmospheric measurements and NIST databases. The model uses an algorithm that distinguishes between continuum and non-continuum regimes based on the local Kn.

1.5   Brief Overview of Thesis Contents

An introduction to research topic has been presented in this chapter. In chapter two, in order to simplify the research problem, first, a neutral thermosphere is assumed. A framework to study dispersion and attenuation of infrasound is then developed. The results obtained based on the continuum and the non-continuum mechanics are compared. In chapter three, the effects of charged thermosphere are considered within the approximation of a PIP via equations of a single-fluid MHD. Also in chapter three, the direct physical method to obtain the attenuation coefficient of acoustic waves is employed. This is done via the Energy Dissipation Corollary (EDC) (Pierce, 1981), which is based on the energy balance equation expressed in conservative form. Chapter four contains conclusions reached based on results of this study and recommendations for direction of future work.

Chapter 2: Modeling Dispersion and Absorption for a Neutral Lower Thermosphere

Better predictions are needed for acoustic attenuation and dispersion in Earth's lower thermosphere. The motivation for this study is that, in the tenuous environment of the lower thermosphere, Kn can become large enough to preclude treating the atmosphere as a continuum. Therefore, the Navier-Stokes (NS) equations are likely to yield erroneous results; one must resort instead to non-continuum fluid mechanics. The latter is made possible through the BTE. The Chapman-Enskog expansion of the BTE to first order in Kn yields the NS equations, and to second order the Burnett (BU) equations. The progression can go on to account for higher-order departures from equilibrium (e.g. 13-moment).

2.1 The NS Stress Tensor and Heat Flux

To obtain the equations describing the motion of a viscous fluid, it is necessary to include terms due to viscosity (internal friction) in the equation of motion of an ideal fluid. The NS stress tensor is defined as (Landau and Lifshitz, 1959):

$$\sigma_{ij} = -p\delta_{ij} + \mu\left(\frac{\partial v_i}{\partial x_j} + \frac{\partial v_j}{\partial x_i} - \frac{2}{3}\delta_{ij}\frac{\partial v_l}{\partial x_l}\right) + \xi\delta_{ij}\frac{\partial v_l}{\partial x_l} \qquad 2.1$$

In tensor notation equation 2.1 can be written as follows:

$$\overleftrightarrow{\sigma} = -p\overleftrightarrow{I} + \mu\left[\nabla\vec{v} + (\nabla\vec{v})^T - \frac{2}{3}\overleftrightarrow{I}\nabla\cdot\vec{v}\right] + \xi\overleftrightarrow{I}\nabla\cdot\vec{v} \qquad 2.2$$

In the NS framework, the heat flux is simply the Fourier law of heat conduction (Mason, 1965) shown below:

$$\vec{q} = -\kappa\nabla T \qquad 2.3$$

In the NS approximation, the stress tensor and heat flux are independent.

2.2 The BU Stress Tensor and Heat Flux

The third order solutions to BTE yields the BU stress tensor and heat flux (Mason, 1965).

$$\overleftrightarrow{\sigma} = -p\overleftrightarrow{I} + \mu\left[\left(2 - \frac{2}{3}\overleftrightarrow{I}\right)\left(\nabla \cdot \vec{v} + \epsilon_3 \frac{\mu}{p_0\rho}\nabla^2 p - \frac{3}{5}\epsilon_2 \frac{\kappa}{T_0\rho c_v}\nabla^2 T\right)\right] \qquad 2.4$$

$$\vec{q} = -\kappa\nabla\mathrm{T} - \frac{\rho_0}{5}\frac{\kappa}{\rho c_v}\left(3\epsilon_1 \frac{\kappa}{\rho c_v} - 4\epsilon_2 \frac{\mu}{\rho}\right)\nabla^2\vec{v} \qquad 2.5$$

In the non-continuum mechanics, the stress tensor and heat flux are no longer independent. The two quantities are coupled. In the BU approximation, the stress tensor depends on the divergence of the pressure gradient force and the divergence of the heat flux. The stress tensor becomes dependent on the thermal properties of the fluid not just on the divergence of the particle velocity as is the case in the NS approximation. Similarly, the BU heat flux becomes dependent on the stress tensor.

2.3 Fluid Transport Equations

At this stage, the thermosphere is assumed to be neutral, hence unaffected by electric and magnetic fields. For simplicity, the effects of gravity are assumed negligible. The equations that govern fluid dynamics are those of mass continuity, conservation of momentum, conservation of energy, and the equation of state. These transport equations are then supplemented by constitutive relations involving the stress tensor and heat flux.

$$\partial_t\rho + \nabla \cdot (\rho\vec{v}) = 0 \qquad 2.6a$$

$$\rho D_t\vec{v} = \nabla \cdot \overleftrightarrow{\sigma} \qquad 2.7a$$

$$\rho D_t U - \overleftrightarrow{\sigma}(\nabla \cdot \vec{v}) + \nabla \cdot \vec{q} = 0 \qquad 2.8a$$

$$\rho = \rho(p, T) \qquad 2.9a$$

10

2.3.1 The Linear Acoustics Approximation

In the linear acoustics regime, fluctuations are assumed to be much less than ambient values. In order to simplify this model, the effect of winds is not considered. The set of fluid transport equations is solved for the wave number at each altitude. The gradient of ambient density is considered insignificant (consistent with neglecting gravity). Linearizing equations 2.6a to 2.9a i.e. keeping terms of order one (O-1) in fluctuating quantities yields the following equations:

$$\partial_t \rho_1 + \rho_0 \nabla \cdot \vec{v}_1 = 0 \tag{2.6b}$$

$$\rho_0 \partial_t \vec{v}_1 = \nabla \cdot \overleftrightarrow{\sigma}_1 \tag{2.7b}$$

$$\rho_0 \partial_t U_1 + p_0 \nabla \cdot \vec{v}_1 + \nabla \cdot \vec{q}_1 = 0 \tag{2.8b}$$

$$\rho_1 = \left(\frac{\partial \rho}{\partial p}\right)_T \delta p + \left(\frac{\partial \rho}{\partial T}\right)_p \delta T = \rho_0 \beta_T p_1 - \rho_0 \propto_p T_1 \tag{2.9b}$$

The internal energy in equation 2.8b can be expanded as follows:

$$U = U(T, \rho)$$

$$U_1 = \left(\frac{\partial U}{\partial T}\right)_\rho \delta T + \left(\frac{\partial U}{\partial \rho}\right)_T \delta \rho = c_v T_1 + \left(\frac{\partial U}{\partial \rho}\right)_T \delta \rho \tag{2.10}$$

Applying the thermodynamic identity (Condon and Odishaw, 1967) with $p \approx p_0$ and $\rho \approx \rho_0$

$$c_p - c_v = \propto_p \left[\frac{p}{\rho} - \rho \left(\frac{\partial U}{\partial \rho}\right)_T\right] \Rightarrow \left(\frac{\partial U}{\partial \rho}\right)_T = \frac{1}{\rho_0}\left(\frac{p_0}{\rho_0} - \frac{c_p - c_v}{\propto_p}\right)$$

$$U_1 = c_v T_1 + \frac{1}{\rho_0}\left(\frac{p_0}{\rho_0} - \frac{c_p - c_v}{\propto_p}\right)\rho_1$$

$$\rho_0 c_v \partial_t T_1 + \left(\frac{p_0}{\rho_0} - \frac{c_p - c_v}{\propto_p}\right)\partial_t \rho_1 + p_0 \nabla \cdot \vec{v}_1 + \nabla \cdot \vec{q}_1 = 0 \tag{2.11}$$

Rearranging equation 2.11 and substituting $-\rho_0 \nabla \cdot \vec{v}_1$ for $\partial_t \rho_1$ (2.6b) the following conservation of energy equation is obtained:

$$\rho_0 c_v \partial_t T_1 - \left(\frac{p_0}{\rho_0} - \frac{c_p - c_v}{\propto_p}\right)\rho_0 \nabla \cdot \vec{v}_1 + p_0 \nabla \cdot \vec{v}_1 + \nabla \cdot \vec{q}_1 = 0 \tag{2.12}$$

which reduces to:

$$\rho_0 c_v \partial_t T_1 + \rho_0 \left(\frac{c_p - c_v}{\propto_p}\right) \nabla \cdot \vec{v}_1 + \nabla \cdot \vec{q}_1 = 0 \qquad \text{2.8b}'$$

2.3.2 Divergence of the Perturbed NS Stress Tensor and Heat Flux

Sound propagation in a viscous fluid is accompanied by fluctuations in pressure, temperature, and density. These, in turn, induce oscillations in both the stress tensor and heat flux. The divergence of NS stress tensor and heat flux are derived below. For air, $\xi = 0$. By perturbing the stress tensor to first order in pressure and particle velocity, one obtains:

$$\overleftrightarrow{\sigma}_1 = -p_1 \overleftrightarrow{I} + \mu \left[\nabla \vec{v}_1 + (\nabla \vec{v}_1)^T - \frac{2}{3}\overleftrightarrow{I}\nabla \cdot \vec{v}_1\right]$$

$$\nabla \cdot \overleftrightarrow{\sigma}_1 = -\nabla p_1 \overleftrightarrow{I} + \mu \left[\nabla \cdot \nabla \vec{v}_1 + \nabla \cdot (\nabla \vec{v}_1)^T - \frac{2}{3}\overleftrightarrow{I}\nabla(\nabla \cdot \vec{v}_1)\right]$$

$$\nabla \cdot \nabla \vec{v}_1 \equiv \nabla^2 \vec{v}_1$$

$$\nabla \cdot (\nabla \vec{v}_1)^T = \nabla \vec{v}_1 \cdot \nabla = \nabla(\vec{v}_1 \cdot \nabla) = \nabla(\nabla \cdot \vec{v}_1) = \nabla^2 \vec{v}_1 + \nabla \times \nabla \times \vec{v}_1$$

Assuming no turbulence i.e. $\nabla \times \nabla \times \vec{v}_1 = 0$

$$\nabla \cdot \overleftrightarrow{\sigma}_1 = -\nabla p_1 \overleftrightarrow{I} + \mu \left[2\nabla^2 \vec{v}_1 - \frac{2}{3}\overleftrightarrow{I}\nabla^2 \vec{v}_1\right]$$

$$\nabla \cdot \overleftrightarrow{\sigma}_1 = -\nabla p_1 + \mu \left(2 - \frac{2}{3}\overleftrightarrow{I}\right)\nabla^2 \vec{v}_1 = -i\vec{K}p_1 - \mu \left(2 - \frac{2}{3}\overleftrightarrow{I}\right)K^2 \vec{v}_1 \qquad \text{2.13}$$

Similarly, the divergence of the fluctuation in heat flux can be expressed, in terms of the first-order temperature perturbation, as

$$\nabla \cdot \vec{q}_1 = -\kappa \nabla^2 T_1 = \kappa K^2 T_1 \qquad \text{2.14}$$

Although solutions to above set of equations can be carried out for various wave field geometries (e.g. spherical, cylindrical, guided waves etc.), the essential features of free-space propagation are retained for plane waves (Mason, 1965). Assuming plane wave solutions to

fluctuating parameters implies inserting 2.13 and 2.14 into 2.7b and 2.8b respectively, and using the plane wave approximation, the system of equations becomes:

$$-i\omega\rho_1 + i\rho_0\vec{K}\cdot\vec{v}_1 = 0 \qquad\qquad 2.6c$$

$$-i\omega\rho_0\vec{v}_1 = -i\vec{K}p_1 - \mu(2 - {}^2/_3\vec{I})K^2\vec{v}_1 \qquad\qquad 2.7c$$

$$-i\omega\rho_0 c_v T_1 + i\rho_0\left(\frac{c_p - c_v}{\alpha_p}\right)\vec{K}\cdot\vec{v}_1 + \kappa K^2 T_1 = 0 \qquad\qquad 2.8c$$

$$\rho_1 - \rho_0\beta_T p_1 + \rho_0\alpha_p T_1 = 0 \qquad\qquad 2.9c$$

2.3.3 Obtaining the Dispersion Equation

The resulting system of equation is homogeneous in fluctuating quantities and can be written in matrix form as follows:

$$\begin{pmatrix} -i\omega & i\rho_0 K & 0 & 0 \\ 0 & i\omega\rho_0 - 4/3\,\mu K^2 & -i\vec{K} & 0 \\ 0 & i\rho_0(c_p - c_v/\alpha_p)K & 0 & \kappa K^2 - i\omega\rho_0 c_v \\ 1 & 0 & -\rho_0\beta_T & \rho_0\alpha_p \end{pmatrix}\begin{pmatrix} \rho_1 \\ v_1 \\ p_1 \\ T_1 \end{pmatrix} = 0 \qquad 2.15$$

For sound waves $\vec{K}\cdot\vec{v}_1 = Kv_1$ and assuming propagation in one direction i.e. $\vec{I} = 1$. The condition for consistency is the vanishing of the determinant.

$$\begin{vmatrix} -i\omega & i\rho_0 K & 0 & 0 \\ 0 & i\omega\rho_0 - \dfrac{4}{3}\mu K^2 & -iK & 0 \\ 0 & i\rho_0\left(\dfrac{c_p - c_v}{\alpha_p}\right)K & 0 & \kappa K^2 - i\omega\rho_0 c_v \\ 1 & 0 & -\rho_0\beta_T & \rho_0\alpha_p \end{vmatrix} \qquad 2.16$$

The determinant of the matrix yields a characteristic equation of order-four (O-4) in K. This represents the dispersion equation, $\tilde{K} = \tilde{K}(\omega)$. The phase speed (speed of sound, c), and the

13

attenuation coefficient ($\propto$), are obtained, respectively from the real and imaginary parts of the dispersion equation: $\tilde{K} = {}^{\omega}/_{c} + i \propto$.

2.3.4 NS Results for a Neutral Thermosphere

To evaluate the NS model, values for ambient parameters are needed. The next section explains how these values were obtained.

2.3.4.1 Ambient Data for the Thermosphere

Ambient data for pressure, density, temperature and mean free path are extracted from the US Standard Atmosphere 1976 (US 76). US 76 is a document compiled by NOAA, NASA, and USAF. It contains data for the mesosphere and lower thermosphere obtained via rocket and satellite over a complete solar cycle. The following ambient data were extracted from US 76: mean free path (Figure 2), pressure, density, temperature (Figure 3), and the number densities of nitrogen, oxygen, and air. At this stage of the model, air is considered as a mixture of its major constituents i.e. nitrogen, $N_2 (\approx 78\%)$ and oxygen, $O_2 (\approx 21\%)$. Up to about 90 km, the molecular weight of air is fairly constant at about 28% $kg/kmol$. Even though molecular weight of air reduces to about 23% $kg/kmol$ at 160 km, the ratio of N_2 to O_2 can be assumed constant. Thermophysical parameters (ρ_o, c_p, c_v, μ and κ) for N_2 and O_2 were obtained from NIST Chemistry Webbook (http://webbook.nist.gov/chemistry/fluid/). Number densities for the two constituents and air obtained from US 76 were used to derive number ratio/concentration of each constituents. The ratios were then multiplied by the total ambient pressure of air to obtain partial pressures for N_2 and O_2. The partial pressures of N_2 and O_2 along with temperature at every 1 km between 85 to 160 km were used to query the NIST Chemistry Webbook for the thermophysical parameters of interest. The values for

each parameter were then combined in ratio of 0.78 of N_2 and 0.21 of O_2 to form an air mixture of N_2 and O_2. The lower-thermospheric profiles of μ and κ for N_2 - O_2 mixture is shown in Figure 4.
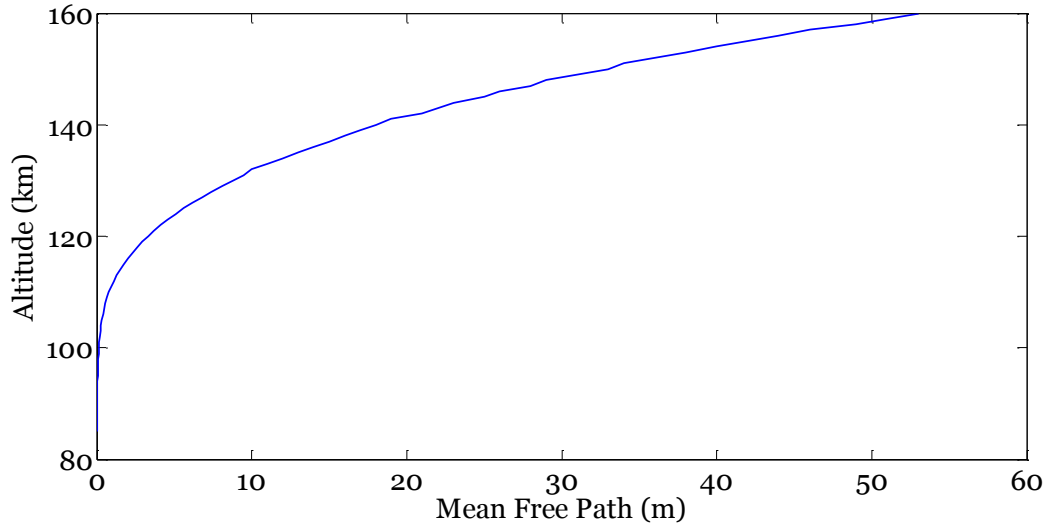
Figure 2: Thermospheric profile of MFP
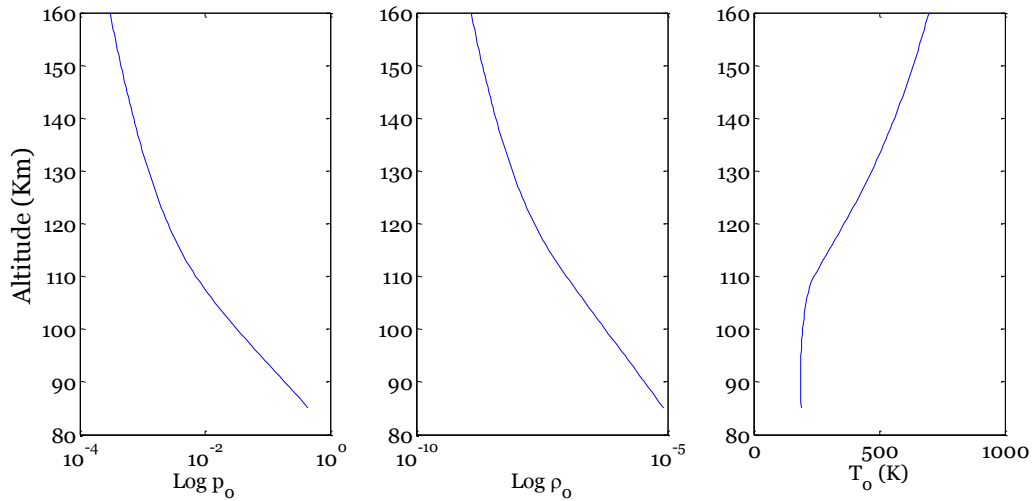
Figure 3: Thermospheric profiles of ambient quantities

15
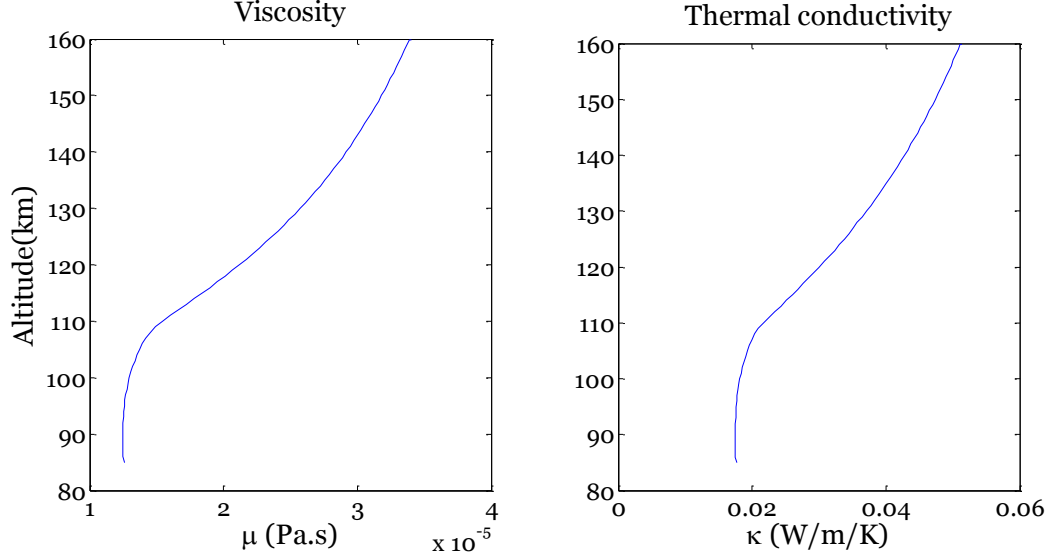
Figure 4: Thermospheric profiles for $N_2 - O_2$ mixture

2.3.4.2 Obtaining the Dispersion Relation

Equation 2.16 is solved using MATLAB for $K(\omega)$ at every 1 km between 85 and 160 km. Thus the dispersion equation is obtained at each altitude. The sound speed and attenuation are obtained from the real and imaginary parts of $\widetilde{K}(\omega)$ as shown below:

$$c(\omega) = \frac{\omega}{Re[\widetilde{K}(\omega)]} \qquad \qquad 2.17a$$

$$\propto (\omega) = Im[\widetilde{K}(\omega)] \qquad \qquad 2.17b$$

The model is evaluated at the following frequencies: 0.01, 0.1, 0.5, 1, 5 and 10 Hz. At every altitude four solutions are obtained for $\widetilde{K}(\omega)$. The physical solutions are the ones having both the real and imaginary part of $\widetilde{K}(\omega)$ positive. Of these, one solution, whose real and imaginary parts are nearly the same, represents an evanescent (or non-propagating) mode. The other physical solution, with the imaginary part smaller than the real part, is the acoustic (or propagating) mode.

16

Alongside sound speed and attenuation profiles, Kn profile is shown. On the Kn profile, the regions within which NS ($Kn < 0.01$) and BU ($Kn > 0.01$) frameworks are each valid are indicated.
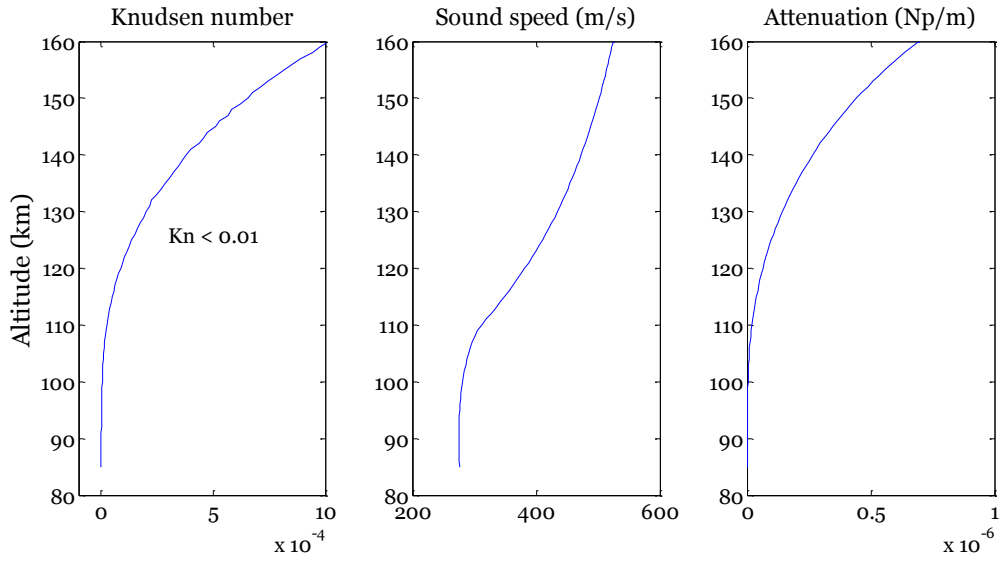
Figure 5: NS model results for 0.01 Hz
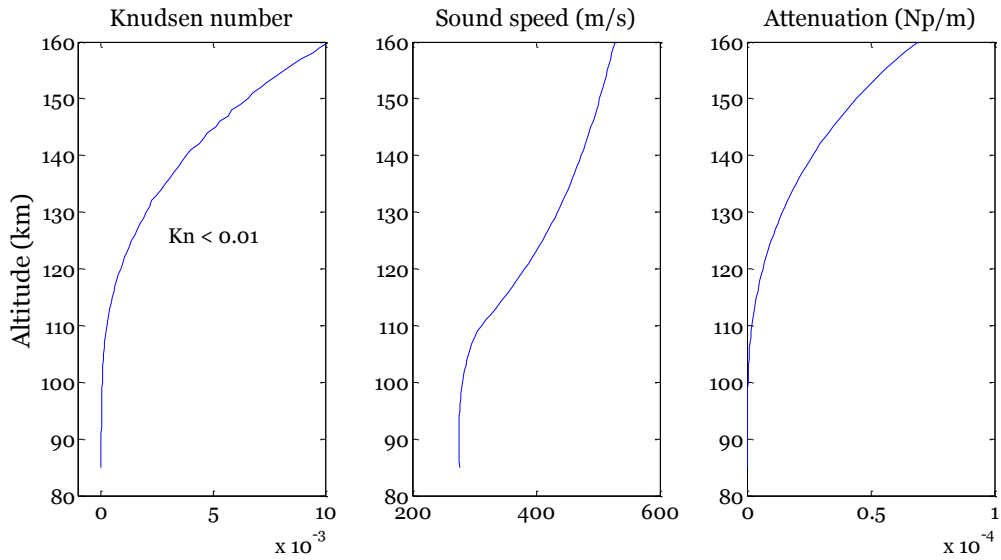
Figure 6: Results of NS model for 0.1 Hz
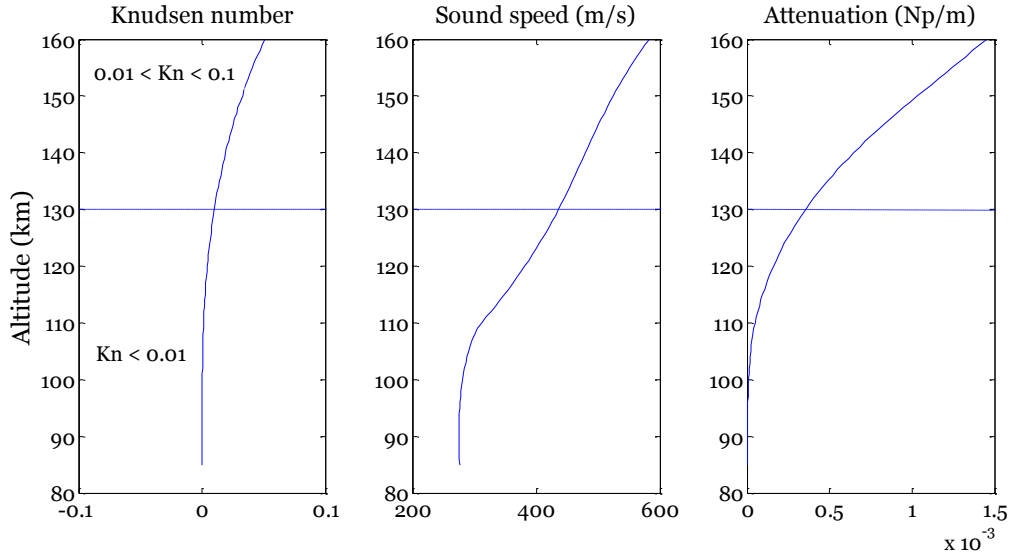
Figure 7: Results of NS model for neutral thermosphere for 0.5 Hz
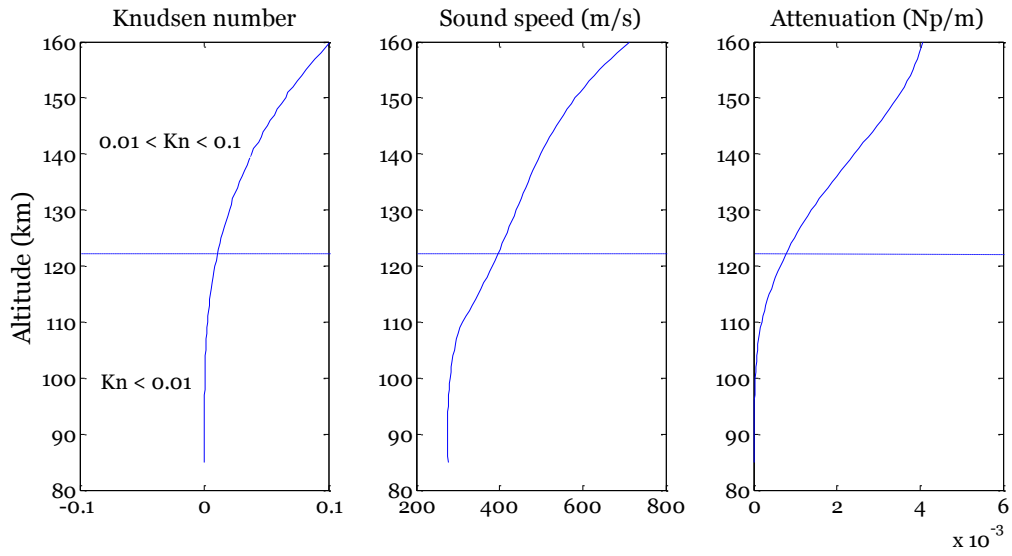
Figure 8: NS model results for 1 Hz

18
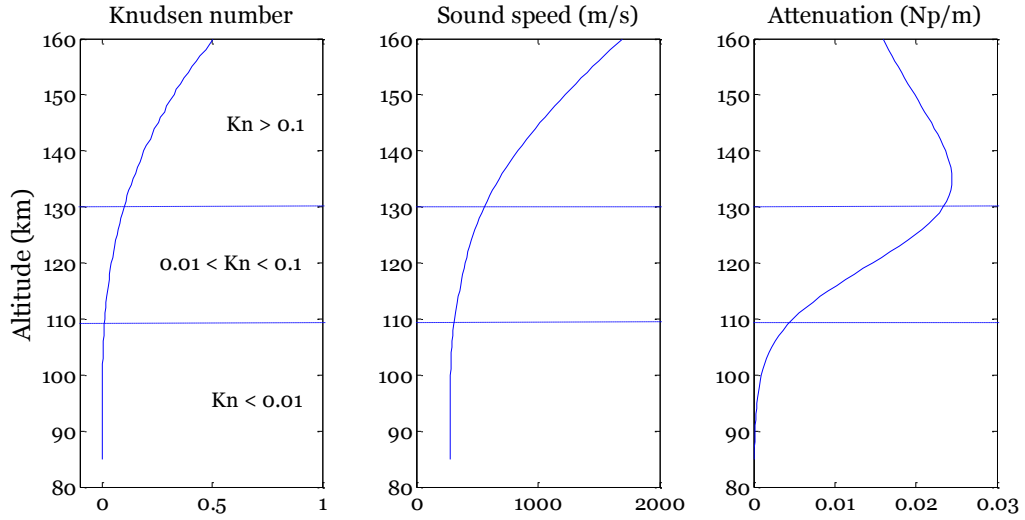
Figure 9: NS model results for 5 Hz
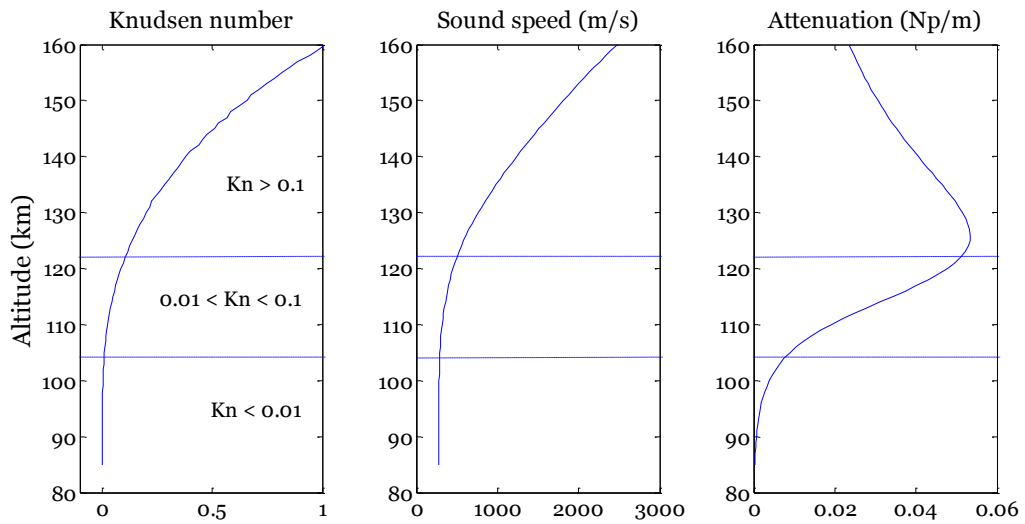
Figure 10: NS model results for 10 Hz

2.3.4.3 Discussion of NS Results

According to theory developed by Stokes and Kirchhoff, the classical attenuation is given by the relation (Landau and Lifshitz, 1959):

$$\propto_{Cl} \cong \frac{\omega^2}{2\rho_0 c_0^3}\left[\frac{4}{3}\mu + (\gamma - 1)\frac{\kappa}{c_p}\right] \qquad 2.18$$

A linear relationship is observed between $\propto_{Cl}$ and μ, similarly between $\propto_{Cl}$ and κ. An expected trend with frequency is observed in $\propto_{Cl}$, with maximum attenuation values been on the order of $10^{-7}(0.01\ Hz), 10^{-5}\ (0.1\ Hz), and 10^{-3}(0.5\ and\ 1\ Hz)$. For a particular altitude, as f increases, λ decreases. This decrease in λ results in an increase in Kn at that particular altitude. The increase in Kn at each altitude as f increase, reduces the height of the region of the thermosphere within which NS approach is most appropriate. The following height boundaries for which NS 'treatment' is most appropriate were noted and shown (represented with dashed line) on Figures 5 to 10. The boundaries are at:

$160\ km\ (0.1\ Hz), 130\ km\ (0.5\ Hz), 122\ km\ (1\ Hz), 109\ km\ (5\ Hz), and\ \ 105\ km\ (10\ Hz)$. Beyond these listed boundaries, the treatment of the thermosphere as a continuum inherent within the NS approach is attributable to the overestimation of infrasound absorption in the lower thermosphere. The appropriate treatment for such regions is non-continuum mechanics inherent within the BU framework, which is described in the following section.

2.4   Burnett Equation Results for a Neutral Thermosphere

The equations for continuity of mass and state remain unchanged. The Burnett stress tensor is inserted in conservation of momentum equation and Burnett heat flux into the conservation of energy equation.

2.4.1 Divergence of the Perturbed BU Stress Tensor and Heat Flux

$$\overleftrightarrow{\delta\sigma} = \overleftrightarrow{\sigma_1} = -\delta p\overleftrightarrow{I} + \mu\left[\left(2 - \frac{2}{3}\overleftrightarrow{I}\right)\left(\nabla\cdot\overrightarrow{\delta v} + \epsilon_3\frac{\mu}{p_0}\delta\left(\frac{\nabla^2 p}{\rho}\right) - \frac{3}{5}\epsilon_2\frac{\kappa}{T_0 c_v}\delta\left(\frac{\nabla^2 T}{\rho}\right)\right)\right] \qquad 2.19$$

Applying the quotient differentiation rule

$$\delta\left(\frac{\nabla^2 p}{\rho}\right) = \frac{\rho\delta(\nabla^2 p) - \nabla^2 p\delta\rho}{\rho^2} = \frac{\rho_0\nabla^2 p_1 + \rho_1\nabla^2 p_1 - \nabla^2 p_0\rho_1 - \nabla^2 p_1\rho_1}{\rho_0^2 + 2\rho_0\rho_1 + \rho_1^2} \qquad 2.20$$

$\rho_1 \ll \rho_0 \Rightarrow \rho_1^2 \approx 0$ and linearizing (keeping terms of order-1 in perturbed quantities)

$$\delta\left(\frac{\nabla^2 p}{\rho}\right) = \frac{\nabla^2 p_1}{\rho_0} - \frac{\rho_1}{\rho_0^2}\nabla^2 p_0 \approx \frac{\nabla^2 p_1}{\rho_0} \ similarly\ \delta\left(\frac{\nabla^2 T}{\rho}\right) \approx \frac{\nabla^2 T_1}{\rho_0} \qquad 2.21$$

Assuming ambient pressure and temperature does not vary appreciably,

$$\overleftrightarrow{\sigma_1} = -p_1 + \mu\left[\left(2 - \frac{2}{3}\overleftrightarrow{I}\right)\left(\nabla\cdot\vec{v}_1 + \epsilon_3\frac{\mu}{p_0}\frac{\nabla^2 p_1}{\rho_0} - \frac{3}{5}\epsilon_2\frac{\kappa}{T_0 c_v}\frac{\nabla^2 T_1}{\rho_0}\right)\right]$$

$$\nabla\cdot\overleftrightarrow{\sigma_1} = -\nabla p_1 + \mu\left[\left(2 - \frac{2}{3}\overleftrightarrow{I}\right)\left(\nabla^2 v_1 + \epsilon_3\frac{\mu}{p_0}\frac{\nabla^3 p_1}{\rho_0} - \frac{3}{5}\epsilon_2\frac{\kappa}{T_0 c_v}\frac{\nabla^3 T_1}{\rho_0}\right)\right] \qquad 2.22$$

Next, the divergence of perturbed heat flux is evaluated.

$$\vec{q} = -\kappa\nabla T - \frac{\rho_0}{5}\frac{\kappa}{\rho c_v}\left(3\epsilon_1\frac{\kappa}{\rho c_v} - 4\epsilon_2\frac{\mu}{\rho}\right)\nabla^2\vec{v} \qquad 2.23$$

$$\vec{q}_1 = -\kappa\nabla T_1 - \frac{\rho_0}{5}\frac{\kappa}{c_v}\left(3\epsilon_1\frac{\kappa}{c_v} - 4\epsilon_2\mu\right)\delta\left(\frac{\nabla^2\vec{v}}{\rho^2}\right)$$

$$\delta\left(\frac{\nabla^2\vec{v}}{\rho^2}\right) = \frac{\rho^2\delta(\nabla^2\vec{v}) - \nabla^2\vec{v}\delta(\rho^2)}{(\rho^2)^2} = \frac{(\rho_0^2 + 2\rho_0\rho_1 + \rho_1^2)\nabla^2 v_1 - (\nabla^2 v_0 + \nabla^2 v_1)2\rho\rho_1}{(\rho_0^2 + 2\rho_0\rho_1 + \rho_1^2)^2}$$

$$\delta\left(\frac{\nabla^2\vec{v}}{\rho^2}\right) \approx \frac{\nabla^2 v_1}{\rho_0^3}$$

$$\vec{q}_1 = -\kappa\nabla T_1 - \frac{\kappa}{5c_v}\left(3\epsilon_1\frac{\kappa}{c_v} - 4\epsilon_2\mu\right)\frac{\nabla^2 v_1}{\rho_0^2}$$

$$\nabla\cdot\vec{q}_1 = -\kappa\nabla^2 T_1 - \frac{\kappa}{5c_v}\left(3\epsilon_1\frac{\kappa}{c_v} - 4\epsilon_2\mu\right)\frac{\nabla^3 v_1}{\rho_0^2} \qquad 2.24$$

In the plane-wave approximation, Equations 2.22 and 2.24 are substituted into 2.7c and 2.8c respectively. The following set of equations is obtained:

$$-i\omega\rho_1 + i\rho_0\vec{K}\cdot\vec{v}_1 = 0 \qquad\qquad 2.6c$$

$$-i\omega\rho_0 v_1 = -iKp_1 + \mu\frac{4}{3}\left(-K^2 v_1 - i\epsilon_3\frac{\mu}{p_0}\frac{K^3 p_1}{\rho_0} + i\epsilon_2\frac{3}{5}\frac{\kappa}{T_0 c_v}\frac{K^3 T_1}{\rho_0}\right) \qquad\qquad 2.7d$$

$$-i\omega\rho_0 c_v T_1 + i\rho_0\left(\frac{c_p - c_v}{\alpha_p}\right)\vec{K}\cdot\vec{v}_1 + \kappa K^2 T_1 + i\frac{\kappa}{5c_v}\left(3\epsilon_1\frac{\kappa}{c_v} - 4\epsilon_2\mu\right)\frac{K^3 v_1}{\rho_0{}^2} = 0 \qquad\qquad 2.8d$$

$$\rho_1 - \rho_0\beta_T p_1 + \rho_0\alpha_p T_1 = 0 \qquad\qquad 2.9c$$

2.4.2 Obtaining the Dispersion Equation

The following matrix determinant is obtained from equations 2.6c, 2.7d, 2.8d and 2.9c:

$$
\begin{vmatrix}
-i\omega & i\rho_0 K & 0 & 0 \\[2ex]
0 & i\omega\rho_0 - \dfrac{4}{3}\mu K^2 & -i\left(K + \dfrac{\mu\epsilon_3 K^3}{\rho_0 p_0}\right) & \dfrac{3i\epsilon_2 \kappa K^3}{5\rho_0 T_0 c_v} \\[2ex]
0 & i\left[\rho_0\left(\dfrac{c_p - c_v}{\alpha_p}\right)K + \left(\dfrac{3\epsilon_1 \kappa^2}{5\rho_0^2 c_v^2} - \dfrac{4\epsilon_2 \mu\kappa}{5\rho_0^2 c_v}\right)K^3\right] & 0 & \kappa K^2 - i\omega\rho_0 c_v \\[2ex]
1 & 0 & -\rho_0\beta_T & \rho_0\alpha_p
\end{vmatrix} \qquad 2.25
$$

Equating matrix determinant 2.25 to zero yields solutions for K.

2.4.2.1 Obtaining the Dispersion Relation

Equation 2.25 is solved using MATLAB for $K(\omega)$ at every 1 km between 85 and 160 km. A complex solution is obtained at each altitude. The sound speed and attenuation are obtained from the real and imaginary parts of $\widetilde{K}(\omega)$ as described in NS model. At every altitude six (6) solutions are obtained for $\widetilde{K}(\omega)$. The physical solution is one with both real and imaginary parts of $\widetilde{K}(\omega)$ positive. Eliminating evanescent modes (commensurate real and imaginary parts), one is left with the acoustic mode (real part larger then imaginary part, as described

in the previous section). The model is evaluated at 0.5 Hz. The resulting sound speed and attenuation profile are shown in Figure 11. Alongside the sound speed and attenuation profiles, the Kn profile is shown. On the Kn profile, the regions within which NS ($Kn < 0.01$) and BU ($Kn > 0.01$) frameworks are assumed to hold are indicated. In region where $Kn < 0.01$, the BU model results converge to NS model results as expected. In the region within which $Kn > 0.01$, a deviation from NS results in sound speed and attenuation profiles is observed. A significant reduction of about 40% in predicted attenuation is observed in the BU profile compared to the NS model at 0.5 Hz. However about 9% increase in predicted sound speed profile is observed in the BU profile compared to the NS model profile.
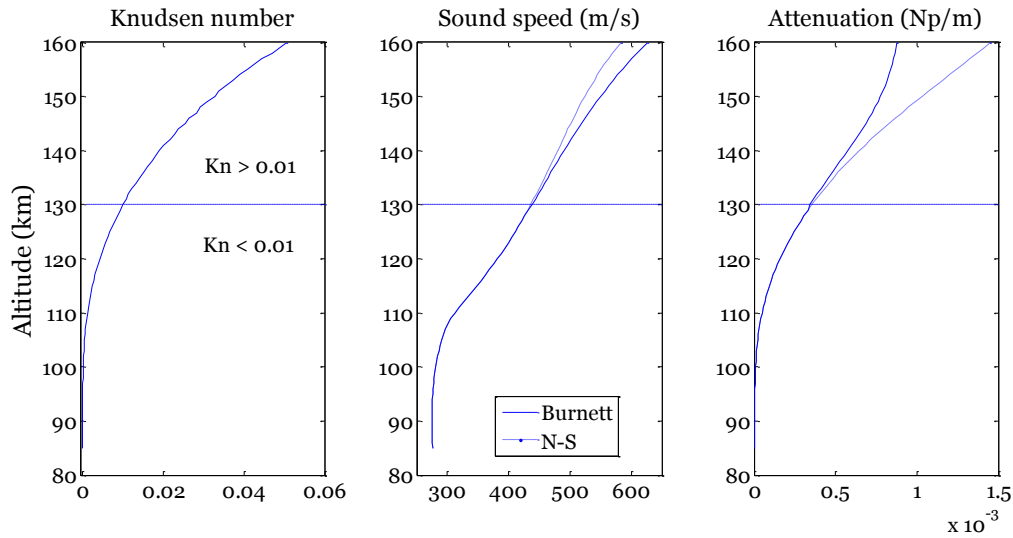
Figure 11: Comparison of Results of BU model to NS model for neutral thermosphere for f = 0.5 Hz

2.5   Rotational Relaxation

Thus far, classical losses have been accounted for in the NS and BU frameworks. This was done by incorporating dissipative effects of viscosity and thermal conductivity. Next, the dissipative effect of molecular relaxation in polyatomic gas components of air is considered. Molecular attenuation are energy losses due to internal degrees of freedom (DOF) of a

molecule, when molecules collide, there is exchange of momentum which results in loss or gain of translational energy of the colliding molecules. However, there is a probability of some collisions resulting in activation of internal DOF. Internal DOF represent rotation of atoms about an axis of the molecule, vibration of atoms about their equilibrium position, and electronic excitation. All the internal DOF are quantized. The amount of energy to activate the rotational DOF is the smallest, that needed for vibrational DOF is larger, while that needed to excite the electronic DOF is the highest. Once a DOF is activated via collisions, the amount of time it takes for the DOF to deactivate, such that the molecule returns to its equilibrium state is known as relaxation time. External/translational DOF relax quasi-instantaneously (via very few collisions) whereas, internal DOF have longer relaxation times (via more collisions). Relaxation processes makes the specific heat capacities of the gas time (or frequency) dependent. This time dependence can be obtained from the energy relaxation equation. Following the partitioning of energy into translational, rotational and vibrational, the specific heat capacity of a gas can also be partitioned similarly. The contribution of vibrational relaxation of N_2 is not considered in this work since it was shown by Bass and Sutherland to contribute negligibly to the heat capacity at lower-thermospheric conditions. At thermospheric altitudes, classical plus rotational relaxation losses reaching maximum values within 80 to 160 km (Sutherland and Bass, 2004).

$$\tilde{c}_v^{eff} = c_v^\infty + c_v^{rot}\Gamma \qquad\qquad 2.26$$

$$c_v^{rot}(diatomic) \equiv R_0 = \frac{R}{M} \qquad\qquad 2.27$$

$$c_v^\infty \equiv c_v^0 - c_v^{rot} \qquad\qquad 2.28$$

$$\tilde{c}_v^{eff} = c_v^0 + R_0(\Gamma - 1) \qquad\qquad 2.29$$

where,

$$\Gamma = \frac{1}{1 - i\omega\tau} \qquad\qquad 2.30$$

24

Relaxation times, τ for, N_2 at thermospheric temperatures were extracted from literature, (Riabov, 2000) see Figure 12 below for extracted profile.
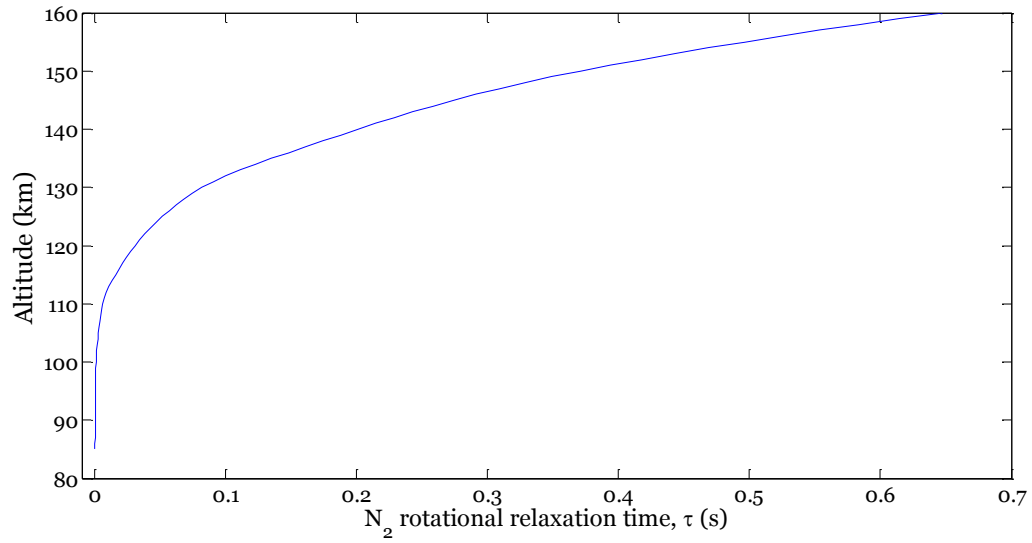
Figure 12: Interpolated (Riabov, 2000) rotational relaxation time for nitrogen gas

2.5.1 Evaluation of Results for the NS and BU Models with Rotational Relaxation

Figure 13 below shows profiles obtained for Kn, sound speed and attenuation for $f = 0.5\ Hz$.
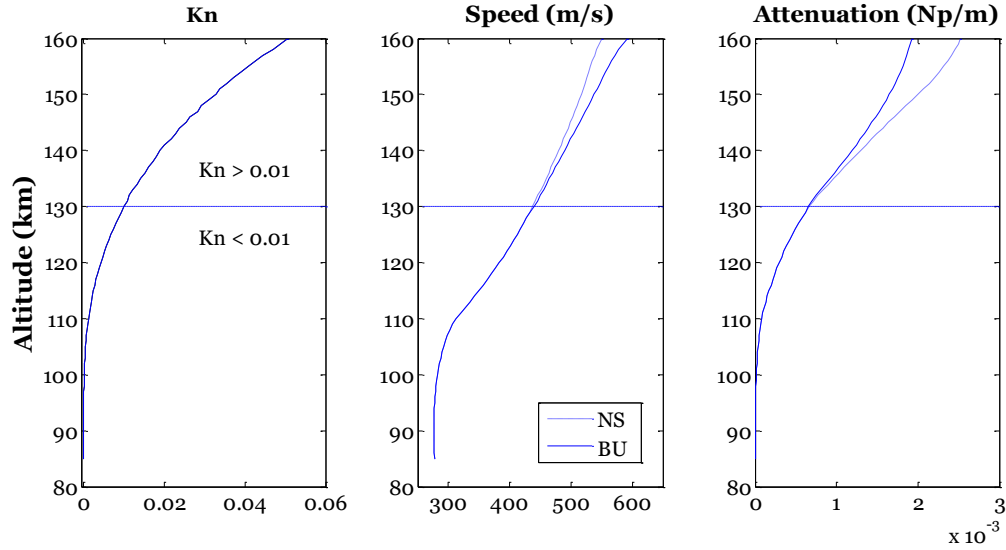
Figure 13: NS-BU results with N_2 rotation relaxation

With the addition of losses due to rotational relaxation of N_2, a significant increase is noted the attenuation profiles for both the NS and BU profiles as expected. Maximum increase of about 67% is observed at 160 km for NS and ~138% for BU. Also, as expected a decrease in sound speed is observed both for the NS and BU profiles.

Chapter 3: Sound Dispersion and Absorption in a Charged Thermosphere

3.1   Composition of the Thermosphere

The ionosphere extends from the mesopause ($\approx 85\ km$) through the thermosphere, into the exosphere ($> 600\ km$). The lower thermosphere overlaps with the E and F_1 ionospheric layers, where charged species coexist with neutrals forming a Partially Ionized Plasma (PIP). The charged species (electrons and positive ions) are produced by two main mechanisms: (1) interaction of solar UV radiation with neutrals and (2) impact of energetic cosmic ray particles. Processes producing charged constituents are reviewed below (Rees, 1989).

3.1.1   Photoionization

This is the principal mechanism by which ions of major thermospheric species are produced. Photoionization reactions and their respective ionization thresholds are as follows:

$$N_2 + h\nu\ (> 15.58\ eV) \rightarrow N_2^+ + e^- \qquad\qquad 3.1$$

$$O_2 + h\nu\ (> 12.08\ eV) \rightarrow O_2^+ + e^- \qquad\qquad 3.2$$

$$O + h\nu\ (> 13.61\ eV) \rightarrow O^+ + e^- \qquad\qquad 3.3$$
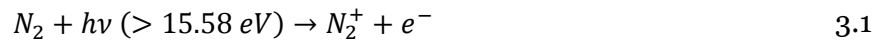
3.1.2   Dissociative Ionization

This reaction produces atomic ions and atomic nitrogen and oxygen and requires more energetic solar photons.

$$O_2 + h\nu\ (> 18.73\ eV) \rightarrow O^+ + O + e^- \qquad\qquad 3.4$$

$$N_2 + h\nu\ (24.32\ eV) \rightarrow N^+ + N + e^- \qquad\qquad 3.5$$
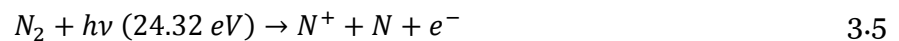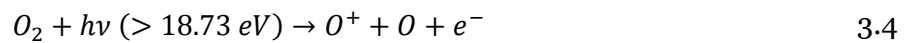
3.2   Acoustic Wave Motion in the Charged Thermosphere

Any attempt to model the dispersion and attenuation of sound waves in the thermosphere should account for the presence of charged species in the thermosphere. Conceptually, the mechanism can be summarized as follows: an acoustic wave front incident from the neutral mesosphere encounters "streams" of charged particles (electrons and ions) traveling along paths defined by existing magnetic and electric fields. Consequently, there will be a collisional exchange of energy between the neutral particles and the charge carriers. This exchange affects the dynamics of the PIP: the charged "streams" are perturbed by the incident acoustic wave motion and, in turn, the acoustic wavefront will lose some coherence. The former effect imposes fluctuations in the electron and ion current densities, as well as electric and magnetic fields. The latter effect embodies the net loss of energy, whose "imprint" is carried, upon downward refraction at the thermospheric inversion, to the ground detector.

A rigorous plasma dynamics model will include separate treatment of neutral-neutral, charged-charged, and charged-neutral interactions. The dynamics of neutral species has been studied in the previous chapter. The dynamics of the electrons and ions can each be described by a set of equations similar to those of neutrals, with addition of the Lorentz force, work done by electro-magnetic forces, Maxwell's equations, and Ohm's law. This approach results in three set of equations for a multi-species plasma which is difficult to solve under most circumstances (Schunk and Nagy, 2009). For this project, however, an effective-fluid approximation is used, within the framework of single-fluid magnetohydrodynamics (1F-MHD). The next sections contain the detailed description of the MHD modeling framework leading to the plane-wave linear dispersion equation.

3.2.1 Single-fluid MHD

The simplest way to approach this problem is to think of the PIP as a single conducting fluid which is electrically neutral (Gartenhaus, 1964). To treat a gas mixture as a single conducting fluid, it is necessary to add the contributions of the individual species and obtain both total and average parameters for the gas mixture (Schunk and Nagy, 2009). These quantities are mass density, charge density, drift velocity, and current density.

$$\rho = \sum_\alpha n_\alpha m_\alpha = n_e m_e + n_i m_i + n_n m_n \qquad\qquad 3.8$$

$$\rho_c = \sum_\alpha n_\alpha e_\alpha = n_e e_s + n_i e_i \qquad\qquad 3.9$$

$$\vec{v} = \sum_\alpha n_\alpha m_\alpha \vec{v}_\alpha \Big/ \sum_\alpha n_\alpha m_\alpha = \frac{n_e m_e \vec{v}_e + n_i m_i \vec{v}_i + n_n m_n \vec{v}_n}{\rho} \qquad\qquad 3.10$$

$$\vec{J} = \sum_\alpha n_\alpha e_\alpha \vec{v}_\alpha = e(n_i \vec{v}_i - n_e \vec{v}_e) \qquad\qquad 3.11$$

Single-fluid mass continuity, and conservation of momentum and energy are derived simply by summing individual equations over all species present in the plasma. To these dynamical equations, we add the equation of state, Maxwell's equations, and the generalized Ohm's law. 1F-MHD equations are listed below:

$$\partial_t \rho + \nabla \cdot (\rho \vec{v}) = 0 \qquad\qquad 3.12$$

$$\rho D_t \vec{v} = \nabla \cdot \vec{\sigma} + \rho \vec{g} + \rho_c \vec{E} + \vec{J} \times \vec{B} \qquad\qquad 3.13$$

$$\frac{\rho^\gamma}{\gamma - 1} D_t \left(\frac{p}{\rho^\gamma}\right) = -\vec{\sigma}' : \nabla \vec{v} - \nabla \cdot \vec{q} + \vec{J} \cdot \left(\vec{E} + \vec{v} \times \vec{B}\right) - \rho_c \vec{E} \cdot \vec{v} \qquad\qquad 3.14$$

$$p = \rho R T \qquad\qquad 3.15$$

$$\nabla \cdot \vec{E} = \frac{\rho_c}{\varepsilon_0} \qquad\qquad 3.16$$

$$\nabla \cdot \vec{B} = 0 \qquad\qquad 3.17$$

$$\nabla \times \vec{E} = -\partial_t \vec{B} \qquad\qquad 3.18$$

$$\nabla \times \vec{B} = \mu_0 \left(\vec{J} + \varepsilon_0 \partial_t \vec{E} \right) \qquad \text{3.19}$$

$$\partial_t \vec{J} + \nabla \cdot \left(\vec{v}\vec{J} + \vec{J}\vec{v} \right) + e\nabla \cdot \left(\frac{\vec{P}_i^*}{m_i} - \frac{\vec{P}_e^*}{m_e} \right) - \frac{n_e e^2}{m_e} \left(\vec{E} + \vec{v}_e \times \vec{B} \right) - \frac{n_i e^2}{m_i} \left(\vec{E} + \vec{v}_i \times \vec{B} \right)$$

$$\text{3.20}$$

$$= \frac{e}{m_i} \frac{\delta \vec{M}_i}{\delta t} - \frac{e}{m_e} \frac{\delta \vec{M}_e}{\delta t}$$

Equation 3.20 contains $\vec{v}_e$ and $\vec{v}_i$ instead of the one fluid velocity. In the next section a generalized Ohm's law is derived for the single fluid.

3.2.2 Derivation of a Generalized Ohm's Law

Considering that $m_e \ll m_i$, then the single fluid density is reduced to

$$\rho \approx n_i m_i + n_n m_n \qquad \text{3.21}$$

Similarly, the single fluid velocity reduces to

$$\vec{v} \approx \frac{n_i m_i \vec{v}_i + n_n m_n \vec{v}_n}{\rho} \approx x_i \vec{v}_i + x_n \vec{v}_n$$

$$\vec{v}_i \approx \frac{\vec{v} - x_n \vec{v}_n}{x_i} \qquad \text{3.22}$$

where x_i, x_n are concentrations/ density ratios of ions and neutrals to the total fluid.

$$x_{i,n} = \frac{\rho_{i,n}}{\rho}$$

$$x_i + x_n \approx 1 \Longrightarrow 1 + \frac{x_n}{x_i} \approx \frac{1}{x_i} \qquad \text{3.23}$$

Substituting 3.23 into 3.22

$$\vec{v}_i \approx \frac{\vec{v} - x_n \vec{v}_n}{x_i} \approx \left(1 + \frac{x_n}{x_i} \right) \vec{v} - \frac{x_n}{x_i} \vec{v}_n \qquad \text{3.24}$$

Assuming single ionization only, $n_e = n_i$ and substituting into 3.11, the following expression is found for $\vec{v}_e$

$$\vec{v}_e = \vec{v}_i - \frac{\vec{J}}{n_i e} \tag{3.25}$$

Since $m_e \ll m_i$, then

$$\frac{\vec{P}_i^*}{m_i} \ll \frac{\vec{P}_e^*}{m_e} \tag{3.26}$$

Similarly

$$\frac{n_i e^2}{m_i} \ll \frac{n_e e^2}{m_e} \tag{3.27}$$

Hence 3.20 reduces to

$$\partial_t \vec{J} + \nabla \cdot (\vec{v}\vec{J} + \vec{J}\vec{v}) - \left(\frac{e}{m_e}\right) \nabla \cdot \vec{P}_e^* - \frac{n_e e^2}{m_e}\left[\vec{E} + \left(\vec{v}_i - \frac{\vec{J}}{n_i e}\right) \times \vec{B}\right] = \frac{e}{m_i}\frac{\delta \vec{M}_i}{\delta t} - \frac{e}{m_e}\frac{\delta \vec{M}_e}{\delta t} \tag{3.28}$$

The collision terms time are defined as follow (Schunk and Nagy, 2009):

$$\frac{e}{m_e}\frac{\delta \vec{M}_e}{\delta t} = e n_e \nu_{ei}(\vec{v}_i - \vec{v}_e) = \nu_{ei}\vec{J} \tag{3.29}$$

$$\frac{e}{m_i}\frac{\delta \vec{M}_i}{\delta t} = \frac{e}{m_i}n_i m_i \nu_{ie}(\vec{v}_e - \vec{v}_i) = \frac{e}{m_i}n_e m_e \nu_{ei}(\vec{v}_e - \vec{v}_i) = -\left(\frac{m_e}{m_i}\right)\nu_{ei}\vec{J} \tag{3.30}$$

Here ν_{ie} and ν_{ei} are momentum transfer collision frequencies for ion-electron and electron-ion collisions. The frequencies are not symmetric but instead satisfy the relation 3.31 (Schunk and Nagy, 2009) which has been used to obtain 3.30.

$$n_i m_i \nu_{ie} = n_e m_e \nu_{ei} \tag{3.31}$$

Since $m_e \ll m_i$, then $\left(\frac{m_e}{m_i}\right) \to 0$. Hence, $\frac{e}{m_i}\frac{\delta \vec{M}_i}{\delta t}$ (3.30) i.e. first term on the right-hand size of 3.28 can be safely neglected.

Multiplying equation 3.28 above by $-\frac{m_e}{n_e e^2}$, the following equation is obtained:

$$-\frac{m_e}{n_e e^2}\left[\partial_t \vec{J} + \nabla \cdot (\vec{v}\vec{J} + \vec{J}\vec{v})\right] + \frac{1}{n_e e}\nabla \cdot \vec{P}_e^* + \vec{E} + \vec{v}_i \times \vec{B} - \frac{1}{n_i e}\vec{J} \times \vec{B} = \frac{m_e \nu_{ei}}{n_e e^2}\vec{J} \tag{3.32}$$

$$\sigma_e = \frac{n_e e^2}{m_e \nu_{ei}} \tag{3.33}$$

where σ_e in the above expression is the parallel conductivity of a fully ionized plasma. The time scale of variation of $\vec{J}$ is assumed large i.e. on the order of one period of the infrasound wave, such that $\partial_t \vec{J} \rightarrow 0$. Linearizing the above equation and keeping terms of order 1 in fluctuations causes the divergence $\nabla \cdot (\vec{v}\vec{J} + \vec{J}\vec{v}) = 0$. Hence, 3.32 becomes:

$$\frac{\vec{J}}{\sigma_e} = \frac{1}{n_e e}\left(\nabla \cdot \vec{P}_e^* - \vec{J} \times \vec{B}\right) + \vec{E} + \vec{v}_i \times \vec{B} \qquad 3.34$$

Substituting 3.24 for $\vec{v}_i$ in 3.34, one obtains:

$$\frac{\vec{J}}{\sigma_e} = \frac{1}{n_e e}\left(\nabla \cdot \vec{P}_e^* - \vec{J} \times \vec{B}\right) + \vec{E} + \left(1 + \frac{x_n}{x_i}\right)\vec{v} \times \vec{B} - \frac{x_n}{x_i}\vec{v}_n \times \vec{B} \qquad 3.35$$

$\vec{J} \times \vec{B}$ term contains the Hall effect contribution:

$$\frac{\vec{J} \times \vec{B}}{n_e e} \equiv \frac{J}{\sigma_e}\frac{eB}{m_e \nu_{ei}}\left(\hat{j} \times \hat{b}\right) = \frac{J}{\sigma_e}\frac{\omega_c^e}{\nu_{ei}}\left(\hat{j} \times \hat{b}\right) \qquad 3.36$$

where use has been made of 3.33,

$$\omega_c^e = \frac{e\vec{B}}{m_e} \qquad 3.37$$

When the electron-ion collision frequency (ν_{ei}) is much greater than the electron cyclotron frequency (ω_c^e), the Hall effect is negligible by comparison to the conductivity contribution, $\frac{\vec{J}}{\sigma_e}$. Within the lower-thermospheric region of 85 to 160 km, $\nu_{ei} \sim 10 - 10^2\ s^{-1}$ and $\omega_c^e \approx 10^7\ s^{-1}$. Even when the collision frequency is not large, it is often possible to neglect both the Hall current and pressure tensor terms (Schunk and Nagy, 2009). Under these conditions, 3.35 reduces to:

$$\frac{\vec{J}}{\sigma_e} = \vec{E} + \left(1 + \frac{x_n}{x_i}\right)\vec{v} \times \vec{B} - \frac{x_n}{x_i}\vec{v}_n \times \vec{B} \qquad 3.38$$

Equation 3.38 is Ohm's law for a two-fluid system (consisting of neutrals and ions). Based on the premise that the masses and temperatures of neutrals and ions are comparable

(Figure 15), their velocities can also be assumed to be close. Hence, the two-fluid Ohm's law (3.38) can be further simplified to the generalized one fluid Ohm's law

$$\frac{\vec{J}}{\sigma_e} = \vec{E} + \vec{v} \times \vec{B}$$

3.39

It is worth noting here that the latest assumption $\vec{v}_n \approx \vec{v}$ is a bit forced, even within the simplifying context of 1F-MHD (as opposed to the full-blown plasma dynamics treatment). The two velocities of neutrals, $\vec{v}_n$ and ions, $\vec{v}_i$ are equivalent to neutral winds and ion drifts, respectively, which may differ noticeably on diurnal and/or seasonal time scales. A two-fluid MHD is likely to be more accurate: the neutral-to-ion concentration ratio is then related to the degree of ionization (assuming atoms are singly ionized). Nevertheless, the theoretical framework developed here to predict infrasound dispersion and absorption in a PIP environment is meant to set the stage for future refinement, guided by new measurements.
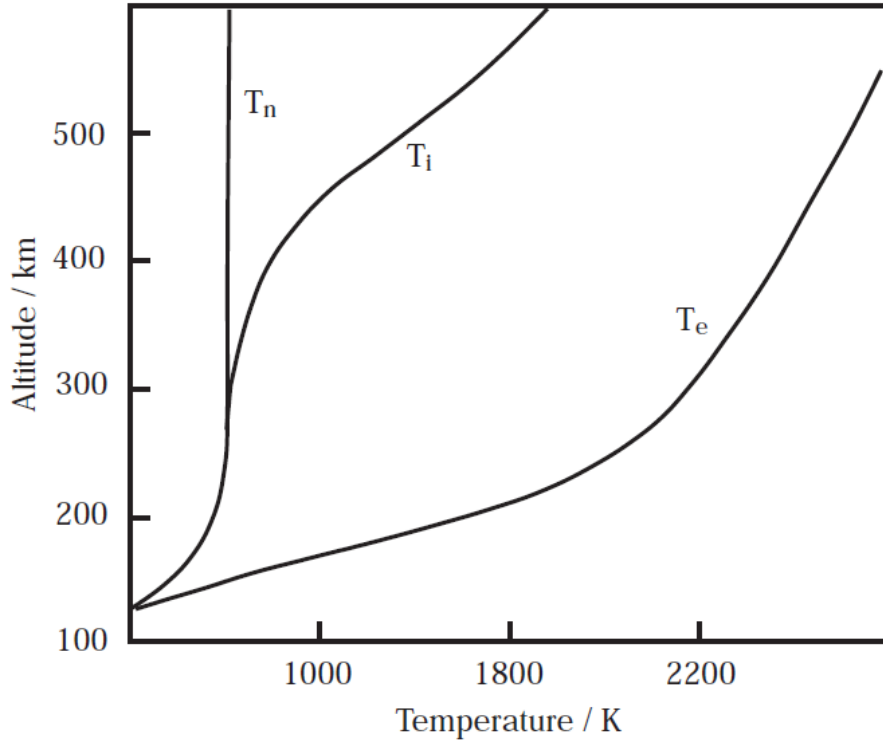
Figure 14: Temperature profiles for electrons, ions and neutrals

3.2.2.1 Conductivity for a PIP

σ_e was defined earlier as the conductivity of a FIP. In this section, σ_e for a PIP is derived. Based on Cowling's three fluid theory, the parallel conductivity for a PIP permeated by magnetic field has been developed (Wang, 1993) as follows:

$$\sigma^{PIP} = \sigma^{FIP} p^{-1} \qquad\qquad 3.40$$

where, p is a function of plasma parameters and it is defined as follows (Wang, 1993):

$$p = 1 + \frac{m_i/v_{ei}}{m_i/v_{en} + 2m_e/v_{in}} \qquad\qquad 3.41$$

Multiply and divide 3.41 by v_{en}/m_i

$$p = 1 + \frac{v_{en}/v_{ei}}{1 + 2m_e/m_i\, v_{en}/v_{in}} \qquad\qquad 3.42$$

Applying the relation (Wang, 1993):

$$\frac{m_e}{m_i}\frac{v_{en}}{v_{in}} \sim \sqrt{\frac{m_e}{m_i}} \qquad\qquad 3.43$$

Since, $m_e \ll m_i$, then $\sqrt{m_e/m_i} \to 0$. Such that 3.42 then becomes:

$$p = 1 + v_{en}/v_{ei} \qquad\qquad 3.44$$

Next, the magnitude of the ratio v_{en}/v_{ei} is examined within the lower thermosphere. Over the range: $85 - 160\ km$, v_{en} ranges from $10^5 - 10^3\ s^{-1}$, while v_{ei} ranges from $10^1 - 10^2\ s^{-1}$. Hence, the ratio: v_{en}/v_{ei} varies from $10^4 - 10$. However, conductivity values used in evaluating the model developed for a charged thermosphere were extracted from atmospheric conductivity profile documented in literature, therefore the factor p is not considered.

3.3 Simplified MHD Equations

At the outset, it is assumed that fluctuations in the electric and magnetic fields are solely the result of the acoustic perturbation. Hence, the variation of E is over the acoustic wave periods, which are relatively long for infrasound. Hence the displacement current in Ampere's law (3.19) can be neglected. Since the plasma is neutral $\rho_c \vec{E} = 0$, similarly $\rho_c \vec{E} \cdot \vec{v}$ and $\nabla \cdot \vec{E} = 0$. The set of equations characterizing the PIP becomes:

$$\partial_t \rho + \nabla \cdot (\rho \vec{v}) = 0 \tag{3.12a}$$

$$\rho D_t \vec{v} = \nabla \cdot \vec{\sigma} + \rho \vec{g} + \vec{J} \times \vec{B} \tag{3.13a}$$

$$\frac{\rho^\gamma}{\gamma - 1} D_t \left(\frac{p}{\rho^\gamma} \right) = -\vec{\sigma}' : \nabla \vec{v} - \nabla \cdot \vec{q} + \vec{J} \cdot \left(\vec{E} + \vec{v} \times \vec{B} \right) \tag{3.14a}$$

$$p = \rho R T \tag{3.15a}$$

$$\nabla \cdot \vec{E} = 0 \tag{3.16a}$$

$$\nabla \cdot \vec{B} = 0 \tag{3.17a}$$

$$\nabla \times \vec{E} = -\partial_t \vec{B} \tag{3.18a}$$

$$\nabla \times \vec{B} = \mu_0 \vec{J} \tag{3.19a}$$

$$\vec{J} = \sigma_e \left[\vec{E} + \left(\vec{v} \times \vec{B} \right) \right] \tag{3.20a}$$

The atmosphere is considered to be windless ($\vec{v}_0 = 0$). Also, for simplicity of the argument, only a geomagnetic ambient field is assumed to be present; no ambient electric field, hence no ambient current density ($\vec{E}_0, \vec{J}_0 = 0$). Assuming no variation in ambient density with time, $\partial_t \rho_0 = 0$. Applying hydrostatic equilibrium $\nabla_0 p_0 = -\rho_0 \vec{g}$. The thermosphere can be divided into sub-layers, each with an average temperature. Hence, within each layer $\nabla_0 T_0 = 0$. Linearizing equations 3.12a to 3.20a:

$$\partial_t \rho_1 + \vec{v}_1 \cdot \nabla_0 \rho_0 + \rho_0 \nabla \cdot \vec{v}_1 = 0 \tag{3.12b}$$

$$\rho_0 \partial_t \vec{v}_1 = -\nabla p_1 + \frac{4}{3} \mu \nabla (\nabla \cdot \vec{v}_1) + \rho_1 \vec{g} + \vec{J}_1 \times \vec{B}_0 \tag{3.13b}$$

34

$$\frac{1}{\gamma - 1}[\partial_t p_1 + \vec{v}_1 \cdot \nabla_0 p_0 + \gamma p_0 (\nabla \cdot \vec{v}_1)] = \kappa \nabla^2 T_1 \qquad \text{3.14b}$$

$$p_0 = \rho_0 R T_0, \qquad c_0^2 = \gamma \frac{p_0}{\rho_0} \ \text{and} \ p_1 = \rho_1 R T_1, \qquad c_0^2 = \frac{p_1}{\rho_1} \qquad \text{3.15b}$$

$$\nabla \cdot \vec{E}_1 = 0 \qquad \text{3.16b}$$

$$\nabla \cdot \vec{B}_0 = 0 \ \text{and} \ \nabla \cdot \vec{B}_1 = 0 \qquad \text{3.17b}$$

$$\nabla \times \vec{E}_1 = -\partial_t \vec{B}_1 \qquad \text{3.18b}$$

$$\nabla \times \vec{B}_0 + \nabla \times \vec{B}_1 = \mu_0 \vec{J}_1 \qquad \text{3.19b}$$

$$\vec{J}_1 = \sigma_e (\vec{E}_1 + \vec{v}_1 \times \vec{B}_0) \qquad \text{3.20b}$$

3.3.1 Hydrostatic Equilibrium

Expressions are sought for terms: $\vec{v}_1 \cdot \nabla_0 \rho_0$ in 3.12b and $\vec{v}_1 \cdot \nabla_0 p_0$ in 3.14b.

$$\nabla_0 p_0 = -\rho_0 \vec{g} \qquad \text{3.45}$$

Atmospheric pressure varies exponentially with altitude as follows:

$$p_0(z) = p_0(0) exp^{-z/H_0} \qquad \text{3.46}$$

where H_0 is scale height defined as:

$$H_0 = \frac{RT_0}{g}$$

$$\vec{v}_1 \cdot \nabla_0 p_0 = -v_{1z} \frac{p_0}{H_0} \qquad \text{3.47}$$

$\vec{v}_1 \cdot \nabla_0 \rho_0$ in 3.12b is expressed as follows, applying the equation of state 3.15b

$$\vec{v}_1 \cdot \nabla_0 \rho_0 = \frac{\vec{v}_1 \cdot \nabla_0 p_0}{RT_0} \qquad \text{3.48}$$

The variation of g with height i.e. $g = g(z)$ is assumed insignificant, at least within each

isothermal layer. Assuming plane wave propagation:

$$-i\omega \rho_1 + \frac{\vec{v}_1 \cdot \nabla_0 p_0}{RT_0} + i\rho_0 \vec{K} \cdot \vec{v}_1 = 0 \qquad \text{3.12c}$$

$$-i\omega\rho_0\vec{v}_1 = -i\vec{K}p_1 - \frac{4}{3}\mu\vec{K}(\vec{K}\cdot\vec{v}_1) + \rho_1\vec{g} + \vec{J}_1 \times \vec{B}_0 \qquad \text{3.13c}$$

$$-i\omega p_1 - v_{1z}\frac{p_0}{H_0} + i\gamma p_0(\vec{K}\cdot\vec{v}_1) = -\kappa(\gamma-1)K^2 T_1 \qquad \text{3.14c}$$

$$p_0 = \rho_0 R T_0, \qquad c_s^2 = \gamma\frac{p_0}{\rho_0} \ \ and \ p_1 = \rho_1 R T_1, \quad c_s^2 = \frac{p_1}{\rho_1} \qquad \text{3.15c}$$

$$i\vec{K}\cdot\vec{E}_1 = 0 \qquad \text{3.16c}$$

$$i\vec{K}\cdot\vec{B}_1 = 0 \qquad \text{3.17c}$$

$$\vec{K}\times\vec{E}_1 = \omega\vec{B}_1 \implies \vec{B}_1 = \frac{\vec{K}\times\vec{E}_1}{\omega} \qquad \text{3.18c}$$

$$i\vec{K}\times\vec{B}_1 \approx \mu_0\vec{J}_1 \qquad \text{3.19c}$$

$$\vec{J}_1 = \sigma_e(\vec{E}_1 + \vec{v}_1 \times \vec{B}_0) \qquad \text{3.20c}$$

The objective of the next sections is to derive characteristic equation, which depends on vectors $\vec{v}, \vec{K}$ and $\vec{B}_0$.

3.3.2 Evaluating $\vec{J}_1 \times \vec{B}_0$ Term in the Momentum Equation

In this section, an expression is sought for $\vec{J}_1 \times \vec{B}_0$ as a function of $\vec{v}, \vec{K}$ and $\vec{B}_0$. First $\vec{E}_1$ and $\vec{B}_1$ are expressed as functions of $\vec{v}, \vec{K}$ and $\vec{B}_0$.

Substituting 3.18c for $\vec{B}_1$ in 3.19c and substituting 3.20c for $\vec{J}_1$ in 3.19c. 3.19c then becomes:

$$\frac{i\vec{K}\times(\vec{K}\times\vec{E}_1)}{\omega} \approx \mu_0\sigma_e(\vec{E}_1 + \vec{v}_1 \times \vec{B}_0) \qquad \text{3.49}$$

Expanding the LHS of 3.49 via a vector calculus identity and then applying 3.16c,

$$\frac{i\vec{K}\times(\vec{K}\times\vec{E}_1)}{\omega} = \frac{i}{\omega}\left[(\vec{K}\cdot\vec{E}_1)\vec{K} - K^2\vec{E}_1\right] = \frac{-iK^2\vec{E}_1}{\omega} \qquad \text{3.50}$$

Replacing the LHS of 3.49 with 3.50 and collecting like terms, the following expression is found:

$$\vec{E}_1 \approx \frac{-\mu_0 \sigma_e (\vec{v}_1 \times \vec{B}_0)}{\left(\mu_0 \sigma_e + \frac{iK^2}{\omega}\right)} \equiv \frac{i\omega\mu_0 \sigma_e (\vec{v}_1 \times \vec{B}_0)}{(K^2 - i\omega\mu_0\sigma_e)} \tag{3.51}$$

A similar expression is now sought for $\vec{B}_1$, substituting 3.51 into 3.18c

$$\vec{B}_1 = \frac{\vec{K} \times \vec{E}_1}{\omega} \approx \frac{i\mu_0 \sigma_e [\vec{K} \times (\vec{v}_1 \times \vec{B}_0)]}{(K^2 - i\omega\mu_0\sigma_e)}$$

Applying a vector calculus identity to $\vec{K} \times (\vec{v}_1 \times \vec{B}_0)$:

$$\vec{K} \times (\vec{v}_1 \times \vec{B}_0) = (\vec{K} \cdot \vec{B}_0)\vec{v}_1 - (\vec{K} \cdot \vec{v}_1)\vec{B}_0$$

$\vec{B}_1$ becomes

$$\vec{B}_1 = \tilde{A}_B(\sigma_e, \omega)[(\vec{K} \cdot \vec{B}_0)\vec{v}_1 - (\vec{K} \cdot \vec{v}_1)\vec{B}_0] \tag{3.52}$$

$\tilde{A}_B(\sigma_e, \omega)$ is a complex coefficient which characterizes electric conductivity effects

$$\tilde{A}_B(\sigma_e, \omega) = \frac{i\mu_0\sigma_e}{(K^2 - i\omega\mu_0\sigma_e)} = \frac{i}{\left(\frac{K^2}{\mu_0\sigma_e} - i\omega\right)} \tag{3.53a}$$

From 3.19c (applying vector calculus identity), the following expression for $\vec{J}_1 \times \vec{B}_0$ is found

$$\vec{J}_1 \times \vec{B}_0 \approx \frac{i(\vec{K} \times \vec{B}_1) \times \vec{B}_0}{\mu_0} = \frac{1}{i\mu_0}\vec{B}_0 \times (\vec{K} \times \vec{B}_1) = \frac{1}{i\mu_0}[(\vec{B}_0 \cdot \vec{B}_1)\vec{K} - (\vec{B}_0 \cdot \vec{K})\vec{B}_1] \tag{3.54a}$$

Substituting 3.52 for $\vec{B}_1$ in 3.54a

$$(\vec{B}_0 \cdot \vec{B}_1)\vec{K} = \tilde{A}_B[(\vec{K} \cdot \vec{B}_0)(\vec{B}_0 \cdot \vec{v}_1) - (\vec{K} \cdot \vec{v}_1)B_0^2] \tag{3.55a}$$

$$(\vec{B}_0 \cdot \vec{K})\vec{B}_1 = \tilde{A}_B(\vec{B}_0 \cdot \vec{K})[(\vec{K} \cdot \vec{B}_0)\vec{v}_1 - (\vec{K} \cdot \vec{v}_1)\vec{B}_0] \tag{3.56a}$$

Substituting $\vec{B}_0 = B_0\hat{b}_0$

$$(\vec{B}_0 \cdot \vec{B}_1)\vec{K} = \tilde{A}_B B_0^2[(\vec{K} \cdot \hat{b}_0)(\hat{b}_0 \cdot \vec{v}_1) - (\vec{K} \cdot \vec{v}_1)]\vec{K} \tag{3.55b}$$

$$(\vec{B}_0 \cdot \vec{K})\vec{B}_1 = \tilde{A}_B B_0^2(\hat{b}_0 \cdot \vec{K})[(\vec{K} \cdot \hat{b}_0)\vec{v}_1 - (\vec{K} \cdot \vec{v}_1)\hat{b}_0] \tag{3.56b}$$

Substituting 3.55b and 3.56b into 3.54a, the following expression is obtained:

$$\vec{J}_1 \times \vec{B}_0 \approx \frac{\tilde{A}_B B_0^2}{i\mu_0}\{[(\vec{K} \cdot \hat{b}_0)(\hat{b}_0 \cdot \vec{v}_1) - (\vec{K} \cdot \vec{v}_1)]\vec{K} - (\hat{b}_0 \cdot \vec{K})[(\vec{K} \cdot \hat{b}_0)\vec{v}_1 - (\vec{K} \cdot \vec{v}_1)\hat{b}_0]\} \tag{3.54b}$$

$$\vec{J}_1 \times \vec{B}_0 \approx \frac{\tilde{A}_B B_0^2}{i\mu_0} \left\{ [(\vec{K} \cdot \hat{b}_0)(\hat{b}_0 \cdot \vec{v}_1) - (\vec{K} \cdot \vec{v}_1)]\vec{K} - (\vec{K} \cdot \hat{b}_0)^2 \vec{v}_1 + (\hat{b}_0 \cdot \vec{K})(\vec{K} \cdot \vec{v}_1)\hat{b}_0 \right\} \qquad 3.54c$$

Inserting v_A, the following expression is obtained.

$$\vec{J}_1 \times \vec{B}_0 \approx -i\tilde{A}_B \rho_0 v_A^2 \left\{ [(\vec{K} \cdot \hat{b}_0)(\hat{b}_0 \cdot \vec{v}_1) - (\vec{K} \cdot \vec{v}_1)]\vec{K} - (\vec{K} \cdot \hat{b}_0)^2 \vec{v}_1 + (\hat{b}_0 \cdot \vec{K})(\vec{K} \cdot \vec{v}_1)\hat{b}_0 \right\} \qquad 3.57$$

3.3.3   Deriving Expression for p_1 in Term of $\vec{v}, \vec{K} and \vec{B}_0$

An expression for T_1 as a function of p_1 (Landau and Lifshitz, 1959) is:

$$T_1 = \left(\frac{\beta_p T_0}{\rho_0 c_p} \right) p_1 \qquad 3.58$$

Substituting 3.58 for T_1 in 3.14c and applying 3.15c

$$i\omega p_1 = -v_{1z} \frac{p_0}{H_0} + i\rho_0 c_0^2 (\vec{K} \cdot \vec{v}_1) + \kappa(\gamma - 1)K^2 \left(\frac{\beta_p T_0}{\rho_0 c_p} \right) p_1 \qquad 3.59$$

Collecting like terms and applying hydrostatic equilibrium,

$$\left[i\omega - \kappa(\gamma - 1)K^2 \left(\frac{\beta_p T_0}{\rho_0 c_p} \right) \right] p_1 = -\rho_0 g v_{1z} + i\rho_0 c_0^2 (\vec{K} \cdot \vec{v}_1)$$

$$p_1 = \frac{-\rho_0 g v_{1z} + i\rho_0 c_0^2 (\vec{K} \cdot \vec{v}_1)}{\left[i\omega - \kappa(\gamma - 1)K^2 \left(\frac{\beta_p T_0}{\rho_0 c_p} \right) \right]} = \frac{\rho_0}{\omega} \frac{ig v_{1z} + c_0^2 (\vec{K} \cdot \vec{v}_1)}{1 + i \left[\frac{\kappa(\gamma - 1)K^2}{\omega} \left(\frac{\beta_p T_0}{\rho_0 c_p} \right) \right]}$$

$$p_1 = \frac{\rho_0}{\omega} \frac{ig v_{1z} + c_0^2 (\vec{K} \cdot \vec{v}_1)}{\tilde{A}_p(\kappa, \omega)} \qquad 3.60$$

$\tilde{A}_p(\kappa, \omega)$ is a complex coefficient which quantifies thermal effects:

$$\tilde{A}_p(\kappa, \omega) = 1 + i \left[\frac{\kappa(\gamma - 1)K^2}{\omega} \left(\frac{\beta_p T_0}{\rho_0 c_p} \right) \right] \qquad 3.61a$$

3.3.4 Obtaining the Characteristic Equation

Substituting $\vec{g} = -g\hat{z}$ and 3.15c into 3.13c, the following equation is obtained:

$$i\omega\rho_0\vec{v}_1 - \left(i\vec{K} + \frac{g\hat{z}}{c_0^2}\right)p_1 - \frac{4}{3}\mu\vec{K}(\vec{K}\cdot\vec{v}_1) + \vec{J}_1 \times \vec{B}_0 = 0 \qquad 3.62$$

Next, derived expressions for $\vec{J}_1 \times \vec{B}_0$ (3.57) and p_1 (3.60) are substituted into 3.62

$$i\omega\rho_0\boldsymbol{\vec{v}_1} - \left(i\vec{\mathbf{K}} + \frac{g\hat{\boldsymbol{z}}}{c_0^2}\right)\frac{\rho_0}{\omega}\frac{igv_{1z} + c_0^2(\vec{\mathbf{K}}\cdot\vec{v}_1)}{\tilde{A}_p} - \frac{4}{3}\mu\vec{\mathbf{K}}(\vec{\mathbf{K}}\cdot\vec{v}_1) \qquad 3.63$$

$$- i\tilde{A}_B\rho_0 v_A^2\left\{\left[(\vec{\mathbf{K}}\cdot\hat{b}_0)(\hat{b}_0\cdot\vec{v}_1) - (\vec{\mathbf{K}}\cdot\vec{v}_1)\right]\vec{\mathbf{K}} - (\vec{\mathbf{K}}\cdot\hat{b}_0)^2\boldsymbol{\vec{v}_1}\right.$$

$$\left. + (\hat{b}_0\cdot\vec{\mathbf{K}})(\vec{\mathbf{K}}\cdot\vec{v}_1)\boldsymbol{\hat{b}_0}\right\} = 0$$

Collecting terms in $\vec{v}_1$, $\vec{\mathbf{K}}$, $\hat{b}_0$ and $\hat{z}$

$$i\rho_0\left[\omega + \tilde{A}_B v_A^2(\vec{\mathbf{K}}\cdot\hat{b}_0)^2\right]\boldsymbol{\vec{v}_1} - i\rho_0\tilde{A}_B v_A^2(\hat{b}_0\cdot\vec{\mathbf{K}})(\vec{\mathbf{K}}\cdot\vec{v}_1)\boldsymbol{\hat{b}_0} - \frac{\rho_0 g}{c_0^2}\frac{igv_{1z} + c_0^2(\vec{\mathbf{K}}\cdot\vec{v}_1)}{\omega\tilde{A}_p}\hat{\boldsymbol{z}} \qquad 3.64$$

$$- i\rho_0\left\{\frac{igv_{1z} + c_0^2(\vec{\mathbf{K}}\cdot\vec{v}_1)}{\omega\tilde{A}_p} + \frac{4\mu}{i3\rho_0}(\vec{\mathbf{K}}\cdot\vec{v}_1)\right.$$

$$\left. - \tilde{A}_B v_A^2\left[(\vec{\mathbf{K}}\cdot\hat{b}_0)(\hat{b}_0\cdot\vec{v}_1) - (\vec{\mathbf{K}}\cdot\vec{v}_1)\right]\right\}\vec{\mathbf{K}}$$

3.3.5 Significance of Coefficients $\tilde{A}_B$ and $\tilde{A}_p$

In this section, the physical significance of coefficients $\tilde{A}_B(\sigma_e, \omega)$ and $\tilde{A}_p(\kappa, \omega)$ is investigated.

For a highly conductive plasma, i.e. $\sigma_e \to \infty$, then $\tilde{A}_B \to -1/\omega$. Similarly as $\kappa \to \infty$,

imaginary part of $\tilde{A}_p(\kappa, \omega) \to \infty$, which implies a lag between pressure and temperature

fluctuations. For a 'cold' plasma (i.e. a low degree of ionization), as $\sigma_e \to 0$, then $\tilde{A}_B \to 0$

and $\vec{B}_1 \to 0$ implying such a plasma would only sustain electrostatic waves such as plasma

oscillations or ion acoustic waves, depending on ω. As $\kappa \to 0$, $\tilde{A}_p \to 1$. This implies there are no thermal losses, therefore p_1 and T_1 are in phase.

To evaluate the validity of the NS characteristic equation developed for a PIP, we evaluate equation 3.64 for the idealized case of a fully ionized plasma of infinite conductivity ($\sigma_e \to \infty$) neglecting the influence of gravity i.e. $g = 0$ and visco-thermal losses i.e. $\mu, \kappa = 0$. Under these conditions, $\tilde{A}_B = -1/\omega$ and $\tilde{A}_p = 1$:

$$i\rho_0\left[\omega - \frac{1}{\omega}v_A^2(\vec{\mathbb{K}}\cdot\hat{b}_0)^2\right]\vec{v}_1 + \frac{i\rho_0}{\omega}v_A^2(\hat{b}_0\cdot\vec{\mathbb{K}})(\vec{\mathbb{K}}\cdot\vec{v}_1)\hat{b}_0 \qquad 3.65$$

$$-i\rho_0\left\{\frac{c_0^2(\vec{\mathbb{K}}\cdot\vec{v}_1)}{\omega} - \frac{1}{\omega}v_A^2\left[(\vec{\mathbb{K}}\cdot\hat{b}_0)(\hat{b}_0\cdot\vec{v}_1) - (\vec{\mathbb{K}}\cdot\vec{v}_1)\right]\right\}\vec{\mathbb{K}}$$

Rearranging, multiplying 3.65 by $-\omega/i\rho_0$

$$\left[-\omega^2 + v_A^2(\vec{\mathbb{K}}\cdot\hat{b}_0)^2\right]\vec{v}_1 - v_A^2(\hat{b}_0\cdot\vec{\mathbb{K}})(\vec{\mathbb{K}}\cdot\vec{v}_1)\hat{b}_0 \qquad 3.66$$

$$+ \left\{(c_0^2 + v_A^2)(\vec{\mathbb{K}}\cdot\vec{v}_1) - v_A^2(\vec{\mathbb{K}}\cdot\hat{b}_0)(\hat{b}_0\cdot\vec{v}_1)\right\}\vec{\mathbb{K}}$$

Equation 3.66 is a "textbook example" of the dispersion relation [see, for instance, Schunk and Nagy (2009)] for characteristic waves that can propagate in a single component, highly conducting plasma.

3.3.6 Solving the Characteristic Equation in a PIP

Equation 3.64 is the dispersion relation for characteristic waves that can propagate in a PIP. The waves may be classified as electrostatic ($\vec{E}_1 \neq 0, \vec{B}_1 = 0$) or electromagnetic ($\vec{E}_1 \neq 0, \vec{B}_1 \neq 0$) while their polarizations can be longitudinal ($\vec{K} \parallel \vec{v}_1$) or transverse($\vec{K} \perp \vec{v}_1$).

Three modes exist to 3.64 depending on relative direction/orientation of vectors $\vec{v}_1$, $\vec{K}$ and $\hat{b}_0$.

3.3.6.1 Case I: Ordinary/Pure Acoustic Wave $\left(\vec{K} \parallel \vec{v}_1 \text{ and } \vec{K} \parallel \hat{b}_0\right)$

In this mode, the acoustic wave propagates along the lines of the magnetic field as shown in Figure 15 below.
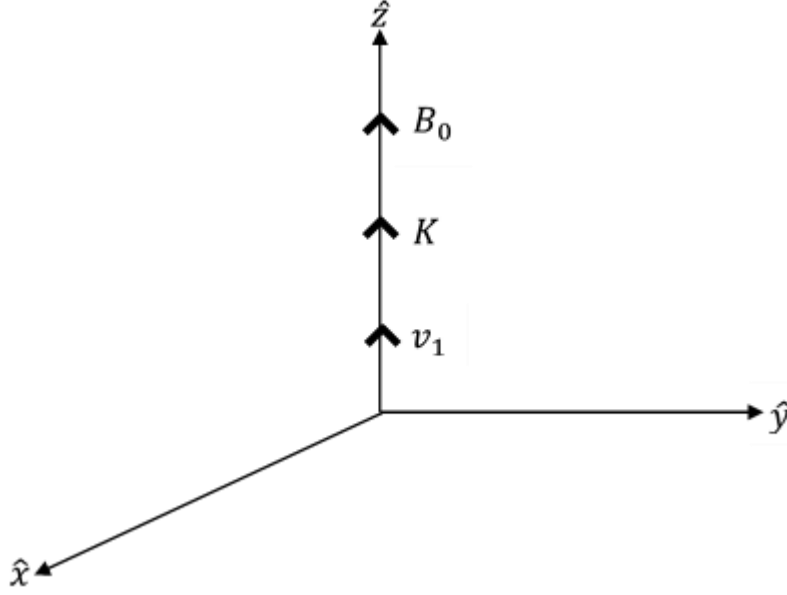
Figure 15: Pure acoustic mode

$$\vec{K} = K\hat{z}, \ \ \hat{b}_0 \equiv \hat{z} \text{ and } \vec{v}_1 = v_{1z}\hat{z} \qquad\qquad 3.67$$

$$\vec{K} \cdot \hat{b}_0 = K, \vec{K} \cdot \vec{v}_1 = Kv_{1z}, \hat{b}_0 \cdot \vec{v}_1 = v_{1z}$$

Substituting 3.67 into 3.64

$$i\rho_0\left[\omega + \tilde{A}_B v_A^2 K^2\right]v_{1z}\hat{z} - i\rho_0\tilde{A}_B v_A^2 K^2 v_{1z}\hat{z} - \frac{\rho_0 g}{c_s^2}\frac{igv_{1z} + c_0^2 Kv_{1z}}{\omega\tilde{A}_p}\hat{z} \qquad 3.68a$$

$$- i\rho_0\left\{\frac{igv_{1z} + c_0^2 Kv_{1z}}{\omega\tilde{A}_p} + \frac{4\mu}{i3\rho_0}Kv_{1z} + \tilde{A}_B v_A^2[Kv_{1z} - Kv_{1z}]\right\}K\hat{z}$$

which further reduces to

$$-\left(\frac{ic_0^2}{\omega\tilde{A}_p} + \frac{4\mu}{3\rho_0}\right)K^2 + i\left(\omega - \frac{g^2}{\omega c_0^2 \tilde{A}_p}\right) = 0 \qquad 3.68b$$

3.68b can be cast in form of an effective frequency and phase speed of sound as follows:

$$K^2 = \frac{\left[\omega^2 - \frac{g^2}{c_0^2 \tilde{A}_p}\right]}{\left[\frac{c_0^2}{\tilde{A}_p} - i\frac{4\omega\mu}{3\rho_0}\right]}$$

<div align="right">3.68c</div>

For a lossless ($\mu, \kappa = 0$) medium and neglecting gravity i.e. $g = 0$, equation 3.68c reduces to dispersion relation, $K^2 = \omega^2/c_0^2$ for an 'ordinary' acoustic wave (Pierce, 1981) which is found in any acoustic textbook. Substituting for $\tilde{A}_p$, 3.68b can be written explicitly as follows:

$$(i4\mu c_0^2 C_\kappa)K^4 + (4\mu\omega c_0^2 + 3\rho_0\omega c_0^2 C_\kappa + i3\rho_0 c_0^4)K^2 + 3i\rho_0(g^2 - \omega^2 c_0^2) = 0 \qquad 3.68d$$

where

$$C_\kappa = \frac{\kappa(\gamma - 1)\beta_p T_0}{\rho_0 c_p}, \qquad \tilde{A}_p(\kappa, \omega) \equiv 1 + i\left[C_\kappa \frac{K^2}{\omega}\right] \qquad\qquad 3.61b$$

Solving 3.68d analytically for K is tedious, if not impossible. Hence, a numerical solution is sought for K in MATLAB. In evaluating this model, K was calculated by solving the dispersion relation 3.68d at an altitude of 100 km, the following wavenumbers were obtained for $f = 0.5\ Hz$ ($Kn{\sim}0.0002$).

$$\tilde{K}_1 = 0.01110806 + i0.00000952, \Longrightarrow c \approx 283\ ms^{-1}\ \&\ \propto\ \approx 0.083\ dB(km)^{-1} \qquad 3.69$$

$$\tilde{K}_2 = 0.01223192 + i14.27466025, \Longrightarrow c \approx 257\ ms^{-1}\ \&\ \propto\ \approx 123{,}990\ dB(km)^{-1} \qquad 3.70$$

The other two solution are mirror images of the 3.69 and 3.70, with their real and imaginary parts being negative.

3.3.6.2 Case II: Alfvén Wave $\left(\vec{K} \perp \vec{v}_1 \text{ and } \vec{K} \parallel \hat{b}_0 \right)$

In this mode, a transverse wave propagates along the lines of the magnetic field. The wave 'plucks' the magnetic field lines.
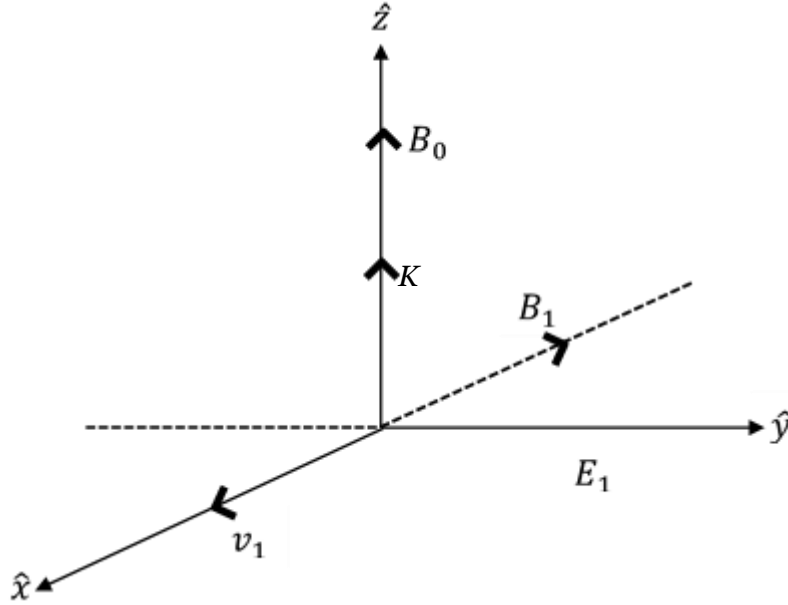
Figure 16: Alfven mode

$$\vec{K} = K\hat{z}, \quad \hat{b}_0 \equiv \hat{z} \text{ and } \vec{v}_1 = v_1\hat{x} \quad v_{1z} = 0 \qquad \text{3.71}$$

$$\vec{K} \cdot \hat{b}_0 = K, \vec{K} \cdot \vec{v}_1 = 0, \hat{b}_0 \cdot \vec{v}_1 = 0$$

Inserting 3.71 into 3.64, the following equation is obtained

$$i\rho_0\left[\omega + \tilde{A}_B v_A^2 K^2\right]v_1\hat{x} = 0 \qquad \text{3.72a}$$

The resulting dispersion relation is

$$\omega + \tilde{A}_B v_A^2 K^2 = 0 \qquad \text{3.72b}$$

3.72b can be cast in terms of frequency and an 'effective' Alfvén wave speed as follows:

$$K^2 = \frac{\omega^2}{-\omega\tilde{A}_B v_A^2} \qquad \text{3.72c}$$

For an idealized ($\sigma_e \rightarrow \infty$) medium, equation 3.72c reduces to dispersion relation, $K^2 = \omega^2/v_A^2$ for an Alfvén wave (Schunk and Nagy, 2009). Substituting for $\tilde{A}_B$, 3.72c can be written explicitly as follows:

$$(\omega^2 + C_e^2 v_A^4)K^2 - (\omega^2 C_e^2 v_A^2 + i\omega^3 C_e) = 0 \qquad \text{3.72d}$$

where

$$C_e = \mu_0 \sigma_e, \quad \tilde{A}_B(\sigma_e, \omega) = \frac{iC_e}{(K^2 - i\omega C_e)} = \frac{i}{\left(\dfrac{K^2}{C_e} - i\omega\right)} \qquad \text{3.53b}$$

3.72d is solved for K at $100\ km$ for $f = 0.5\ Hz$, the following wavenumber is obtained:

$$\tilde{K} = (1.40684163 + i1.40684163) \times 10^{-6}, \qquad \text{3.73}$$

$$\Longrightarrow v_A \approx 2{,}233{,}981\ ms^{-1}\ \&\ \propto\ \approx 0.012\ db(km)^{-1}$$

This solution represents an evanescent mode (non-propagating). The Alfvén wave is an electromagnetic wave which is not the focus of this work. Next, the characteristic equation 3.64 is evaluated for the magnetosonic wave.

3.3.6.3 Case III: Magnetosonic Wave $\left(\vec{K} \parallel \vec{v}_1 \text{ and } \vec{K} \perp \hat{b}_0 \right)$

In this mode, the acoustic wave propagates perpendicularly to the magnetic field lines, causing compression and rarefaction of the magnetic field lines.
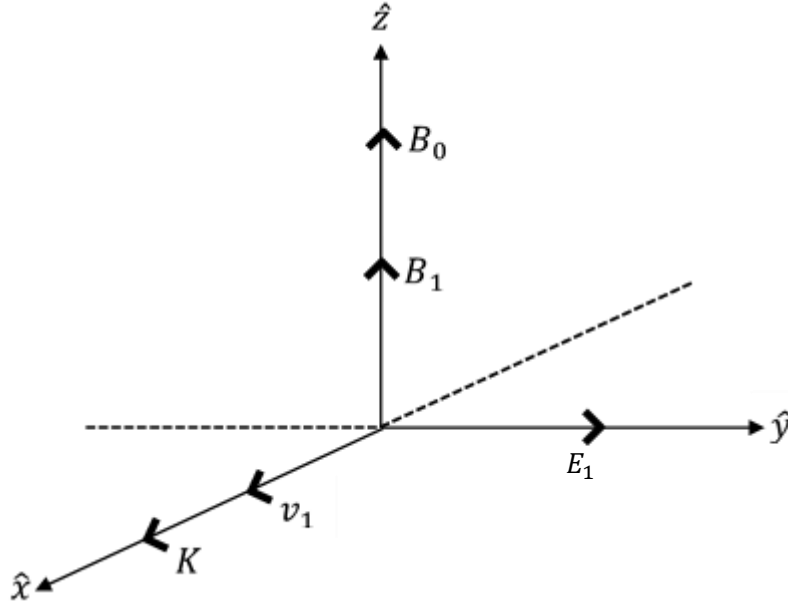

Figure 17: Magnetosonic mode

$$\vec{K} = K\hat{x}, \quad \hat{b}_0 \equiv \hat{z} \text{ and } \vec{v}_1 = v_1\hat{x} \quad v_{1z} = 0 \tag{3.74}$$

$$\vec{K} \cdot \hat{b}_0 = 0, \vec{K} \cdot \vec{v}_1 = Kv_1, \hat{b}_0 \cdot \vec{v}_1 = 0$$

Inserting 3.74 into 3.64

$$i\rho_0\omega v_1\hat{x} - \frac{\rho_0 g K v_1}{\omega \tilde{A}_p}\hat{z} - i\rho_0\left[\frac{c_0^2}{\omega \tilde{A}_p} + \frac{4\mu}{i3\rho_0} - \tilde{A}_B v_A^2\right]K^2 v_1\hat{x} \tag{3.75}$$

From 3.75, two dispersion relations are obtained. The first is:

$$-\frac{\rho_0 g K}{\omega \tilde{A}_p} = 0 \tag{3.76a}$$

substituting 3.61a into 3.75a, the following representation of 3.75a is obtained

$$\left[\kappa(\gamma - 1)\beta_p T_0\right]K^2 + i\omega\rho_0 c_p = 0 \tag{3.76b}$$

For a lossless medium($\kappa = 0$), $K = 0$. However, for a thermal ($\kappa \neq 0$) medium, the following wavenumber is obtained at an altitude of $100 \ km$ for $f = 0.5 \ Hz$:

45

$$\widetilde{K} = 0.35193443 - i0.35193443, \Longrightarrow c \approx 9 \, ms^{-1} \, \& \, \propto \approx 3057 \, db(km)^{-1} \qquad 3.77$$

This represents a non-propagating 'thermal-like' mode considering that its occurrence solely depends on $\kappa \neq 0$. Hence $c \approx 9 \, m/s$ is not a sound speed but a thermal wave speed. The second magnetosonic dispersion relation obtained from 3.75 is

$$-\left[\frac{c_0^2}{\omega \tilde{A}_p} + \frac{4\mu}{i3\rho_0} - \tilde{A}_B v_A^2\right]K^2 + \omega = 0 \qquad 3.78a$$

3.78a can be cast in terms of frequency and an 'effective' magnetosonic wave speed as follows:

$$K^2 = \frac{\omega^2}{\left[\frac{c_0^2}{\tilde{A}_p} + \frac{4\omega\mu}{i3\rho_0} - \omega\tilde{A}_B v_A^2\right]} \qquad 3.78b$$

For a lossless ($\mu, \kappa = 0$) and ideal ($\sigma_e \rightarrow \infty$) medium, equation 3.78b reduces to dispersion relation, $K^2 = \omega^2/(c_0^2 + v_A^2)$ for a magnetosonic wave (Schunk and Nagy, 2009).

3.78a can also be expressed as follows:

$$-i4\mu C_\kappa K^6 - [i3\rho_0(v_A^2 C_\kappa C_e + c_0^2) + 4\mu\omega(1 + C_\kappa C_e) + 3\omega\rho_0 C_\kappa]K^4 \qquad 3.78c$$

$$+ [i3\omega^2\rho_0(1 + C_\kappa C_e) + i4\mu\omega^2 C_e - 3\omega\rho_0 C_e(c_0^2 + v_A^2)]K^2 + 3\omega^3\rho_0 C_e = 0$$

3.78c is solved for K at $100 \, km$, and the following wavenumbers are obtained:

$$\widetilde{K}_1 = 0.01110806 + i0.00000952, \Longrightarrow c \approx 283 \, ms^{-1} \, \& \, \propto \approx 0.083 \, dB(km)^{-1} \qquad 3.79$$

$$\widetilde{K}_2 = 0.01223192 + i14.27466025, \Longrightarrow c \approx 257 \, ms^{-1} \, \& \, \propto \approx 123,990 \, dB(km)^{-1} \qquad 3.80$$

$$\widetilde{K}_3 = 0.00000079 + i0.00000079, \Longrightarrow c \approx 3,978,300 \, ms^{-1} \, \& \, \propto \approx 0.007 \, dB(km)^{-1} \qquad 3.81$$

The first two solutions are same as those of the pure acoustic mode, while the third is an evanescent 'electromagnetic-like' wave.

3.3.6.4 Case IV: $\left(\vec{K} \perp \vec{v}_1, \ \vec{K} \perp \hat{b}_0 \text{ and } \hat{b}_0 \perp \vec{v}_1\right)$

For this case, $\vec{K} \cdot \hat{b}_0 = 0, \vec{K} \cdot \vec{v}_1 = 0, \hat{b}_0 \cdot \vec{v}_1 = 0$ and $v_{1z} = 0$. Under these conditions, 3.64

reduces to trivial solution, $\omega = 0$.

3.4   Acoustics Energy Loss Mechanism

In this section, the acoustic absorption in the presence of ambient and fluctuating magnetic

fields is sought explicitly as intensity losses. The goal here is to estimate the additional

absorption occurring when work is done by the wave to cause magnetic field perturbations.

This approach is, at this stage, speculative: it represents a preliminary basis for extending

the "usual" treatment of intensity dissipation--based on thermo-viscous losses--to include

electro-magnetic effects. Considering a medium with small viscosity and thermal

conductivity, the direct method is to obtain the attenuation coefficient of acoustic waves via

the Energy Dissipation Corollary (EDC), based on the energy balance equation expressed in

conservative form (Pierce, 1981):

$$\partial_t w + \nabla \cdot \vec{I} = -\mathrm{D} \qquad\qquad 3.82$$

The terms are defined as follows:

$\partial_t w$ is the time rate of change of acoustic energy, w.

$\nabla \cdot \vec{I}$ is the net rate of outflow of acoustic energy through surface area of the fluid volume.

$\vec{I} = p\vec{v}$ is the acoustic intensity measured in Wm^{-2}.

D is the acoustic energy dissipated per unit volume and time.

3.4.1 The Magneto-fluid Stress Tensor

In order to account for the effect of electric and magnetic forces, the Maxwell stress tensor is added to the fluid stress tensor (previously defined). Since the plasma is neutral, only the magnetic contribution to Maxwell stress tensor is considered.

$$\sigma_{ij} = \sigma_{ij}^{visc} + \sigma_{ij}^{mag} = -p\delta_{ij} + \sigma_{ij}' - \frac{B^2}{2\mu_0}\delta_{ij} + \frac{B_i B_j}{\mu_0}$$

collecting like terms, the following representation is obtained:

$$\sigma_{ij} = \sigma_{ij}^{visc} + \sigma_{ij}^{mag} = -\left(p + \frac{B^2}{2\mu_0}\right)\delta_{ij} + \mu\Phi_{ij} + \frac{B_i B_j}{\mu_0} \qquad \text{3.83}$$

Expanding the 1st term of 3.83

$$p + \frac{B^2}{2\mu_0} = p_0 + p_1 + \frac{(\vec{B}_0 + \vec{B}_1)^2}{2\mu_0} = \left(p_0 + \frac{B_0^2}{2\mu_0}\right) + \left(p_1 + \frac{\vec{B}_0 \cdot \vec{B}_1}{\mu_0}\right) \qquad \text{3.84}$$

i.e. ambient and perturbed net (i.e. magneto-fluid) pressures, respectively (keeping terms of order 1 in perturbed quantities).

3.4.2 The Momentum Balance Equation

$$\rho_0\,\partial_t \vec{v}_1 \cong \nabla \cdot \overleftrightarrow{\sigma} + \rho\vec{g} = \nabla \cdot \left(\overleftrightarrow{\sigma}^{visc} + \overleftrightarrow{\sigma}^{mag}\right) + \rho_0\,\vec{g} + \rho_1\vec{g} \qquad \text{3.85}$$

The RHS of 3.85 can be expanded by substituting 3.83 and 3.84 as follows:

$$\nabla \cdot \overleftrightarrow{\sigma} + \rho\vec{g} = -\nabla_0\left(p_0 + \frac{B_0^2}{2\mu_0}\right)\overleftrightarrow{I} - \nabla\left(p_1 + \frac{\vec{B}_0 \cdot \vec{B}_1}{\mu_0}\right)\overleftrightarrow{I} + \mu\nabla \cdot \overleftrightarrow{\Phi} + \frac{1}{\mu_0}\left(\nabla \cdot \vec{B}\vec{B}\right) + \rho_0\,\vec{g} + \rho_1\vec{g} \qquad \text{3.86}$$

Applying hydrostatic equilibrium and using vector calculus identities on the magnetic terms, the RHS of Equation 3.86 can be transformed as shown below. For the first magnetic term, $\nabla_0\left(B_0^2/2\mu_0\right) = 0$ because the geomagnetic field is assumed uniform. The second magnetic term in 3.86 becomes:

$$\nabla(\vec{B}_0 \cdot \vec{B}_1) = (\vec{B}_0 \cdot \nabla)\vec{B}_1 + (\vec{B}_1 \cdot \nabla)\vec{B}_0 + \vec{B}_0 \times (\nabla \times \vec{B}_1) + \vec{B}_1 \times (\nabla \times \vec{B}_0) \qquad \text{3.87}$$

$$= (\vec{B}_0 \cdot \nabla)\vec{B}_1 + (\vec{B}_1 \cdot \nabla)\vec{B}_0 + \vec{B}_0 \times (\nabla \times \vec{B}_1)$$

where $\nabla \times \vec{B}_0 = \mu_0 \vec{J}_0 = 0$, since it is assumed that $\vec{E}_0 = 0$. The third magnetic term on the RHS of 3.86 involves the divergence of $\vec{B}\vec{B}$ dyad. The dyad's ij component can be expanded in terms of first-order field fluctuations, as:

$$\frac{1}{\mu_0}(\nabla \cdot \vec{B}\vec{B}) = \frac{1}{\mu_0}\sum_{ij} \hat{e}_i \partial_j \big(B_{0i}B_{0j} + B_{0i}B_{1j} + B_{1i}B_{0j}\big)$$

where terms have been kept to order 1. Since the ambient geomagnetic field is considered uniform.

$$\sum_{ij} \hat{e}_i \partial_j \big(B_{0i}B_{0j}\big) = 0$$

Hence,

$$\frac{1}{\mu_0}(\nabla \cdot \vec{B}_i \vec{B}_j) = \frac{1}{\mu_0}\sum_{ij} \hat{e}_i \partial_j \big(B_{0i}B_{1j} + B_{1i}B_{0j}\big)$$

$$= \frac{1}{\mu_0}\sum_{ij} \hat{e}_i \big(B_{0i}\partial_j B_{1j} + B_{0j}\partial_j B_{1i}\big)$$

$$\frac{1}{\mu_0}\sum_{ij} \hat{e}_i \big(B_{0i}\partial_j B_{1j} + B_{0j}\partial_j B_{1i}\big) = \frac{1}{\mu_0}\big[\vec{B}_0(\nabla \cdot \vec{B}_1) + (\vec{B}_0 \cdot \nabla)\vec{B}_1\big]$$

$$\frac{1}{\mu_0}(\nabla \cdot \vec{B}_i \vec{B}_j) = \frac{1}{\mu_0}\big[\vec{B}_0(\nabla \cdot \vec{B}_1) + (\vec{B}_0 \cdot \nabla)\vec{B}_1\big] \qquad \text{3.88}$$

Conservation of momentum equation (3.85) becomes:

$$\rho_0 \, \partial_t \vec{v}_1 \cong -\nabla p_1 - \frac{1}{\mu_0}\big[(\vec{B}_0 \cdot \nabla)\vec{B}_1 + (\vec{B}_1 \cdot \nabla)\vec{B}_0 + \vec{B}_0 \times (\nabla \times \vec{B}_1)\big] + \mu\nabla \cdot \overleftrightarrow{\Phi}$$

$$\text{3.89a}$$

$$+ \frac{1}{\mu_0}\big[\vec{B}_0(\nabla \cdot \vec{B}_1) + (\vec{B}_0 \cdot \nabla)\vec{B}_1\big] + \rho_1 \vec{g}$$

Hence, 3.89a becomes:

$$\rho_0\, \partial_t \vec{v}_1 \cong -\nabla p_1 - \frac{1}{\mu_0}\left[\vec{B}_0 \times (\nabla \times \vec{B}_1)\right] + \mu\nabla \cdot \overleftrightarrow{\Phi} + +\rho_1\vec{g} \tag{3.89b}$$

$$\rho_0\, \partial_t \vec{v}_1 \cong -\nabla p_1 - \vec{B}_0 \times \vec{J}_1 + \mu\nabla \cdot \overleftrightarrow{\Phi} + +\rho_1\vec{g} \tag{3.89c}$$

where Ampere's law for the magnetic fluctuation was used, in the form:

$$\nabla \times \vec{B}_1 = \mu_0\vec{J}_1$$

3.4.3 The Energy Balance Equation

$$\rho_0 T_0 \partial_t s_1 \cong \nabla \cdot (\kappa\nabla T_1) + \frac{(\vec{B}_0 \cdot \vec{B}_0)(\nabla \cdot \vec{v}_1)}{\mu_0} \tag{3.90}$$

To derive the equation for the conservation of acoustic energy, the following 'recipe' is followed (Pierce, 1981):

$$\vec{v}_1 \cdot Momentum + \left(\frac{p_1 + \dfrac{\vec{B}_0 \cdot \vec{B}_1}{\mu_0}}{\rho_0}\right) Continuity + \left(\frac{T_1}{T_0}\right) Entropy \tag{3.91}$$

First, the LHS of 3.91 is evaluated as follows

$$\vec{v}_1 \cdot \rho_0\, \partial_t \vec{v}_1 + \left(\frac{p_1}{\rho_0} + \frac{\vec{B}_0 \cdot \vec{B}_1}{\mu_0 \rho_0}\right)\partial_t \rho_1 + \frac{T_1}{T_0}\rho_0 T_0 \partial_t s_1 \tag{3.92}$$

Applying product rule to the first term of 3.92 i.e.

$$\partial_t(\vec{v}_1 \cdot \vec{v}_1) = \vec{v}_1 \cdot \partial_t \vec{v}_1 + \partial_t \vec{v}_1 \cdot \vec{v}_1 \implies \vec{v}_1 \cdot \partial_t \vec{v}_1 = \frac{1}{2}\, \partial_t v_1^2 \tag{3.93}$$

Similarly, applying the product rule to second term of 3.92 i.e.

$$\frac{\vec{B}_0 \cdot \vec{B}_1}{\mu_0 \rho_0}\partial_t \rho_1 = \partial_t\left(\frac{\rho_1}{\rho_0}\frac{\vec{B}_0}{\mu_0} \cdot \vec{B}_1\right) - \frac{\rho_1}{\rho_0}\frac{\vec{B}_0}{\mu_0} \cdot (\partial_t \vec{B}_1) \tag{3.94}$$

Substituting 3.93 and 3.94 into 3.92 and substituting p_1/c_0^2 for ρ_1, the LHS of 3.92 becomes:

$$\partial_t\left(\frac{1}{2}\rho_0\, v_1^2\right) + \partial_t\left(\frac{1}{2}\frac{p_1^2}{\rho_0\, c_0^2} + \frac{\rho_0\, T_0}{2c_p}s_1^2\right) + \partial_t\left(\frac{\rho_1}{\rho_0}\frac{\vec{B}_0}{\mu_0} \cdot \vec{B}_1\right) - \frac{\rho_1}{\rho_0}\frac{\vec{B}_0}{\mu_0} \cdot (\partial_t \vec{B}_1) \tag{3.95}$$

50

Next, the RHS of 3.92 is:

$$-\vec{v}_1 \cdot \nabla p_1 + \mu \vec{v}_1 \cdot (\nabla \cdot \overleftrightarrow{\Phi}) - \vec{v}_1 \cdot (\vec{B}_0 \times \vec{J}_1) + \rho_1 \vec{v}_1 \cdot \vec{g} - \left(p_1 + \frac{\vec{B}_0 \cdot \vec{B}_1}{\mu_0}\right) \nabla \cdot \vec{v}_1 + \frac{T_1}{T_0}(\kappa \nabla^2 T_1)$$

$$+ \frac{T_1}{\mu_0 T_0}(\vec{B}_0 \cdot \vec{B}_0)(\nabla \cdot \vec{v}_1)$$

3.96

$$\mu \vec{v}_1 \cdot (\nabla \cdot \overleftrightarrow{\Phi}) \equiv \mu \vec{v}_1 \cdot \sum_{ij} \hat{e}_i \partial_j (\Phi_{ij}) = \frac{4}{3} \mu \vec{v}_1 \cdot \nabla(\nabla \cdot \vec{v}_1)$$

3.97

Applying product rule to the RHS of 3.97, the following equation is obtained.

$$\mu \vec{v}_1 \cdot \sum_{ij} \hat{e}_i \partial_j \Phi_{ij} = \frac{4}{3} \mu \{\nabla \cdot [\vec{v}_1(\nabla \cdot \vec{v}_1)] - (\nabla \cdot \vec{v}_1)^2\}$$

3.98

Applying product rule to sixth term of 3.96, we obtain the following equation.

$$\frac{\kappa}{T_0} T_1 \nabla \cdot (\nabla T_1) = \frac{\kappa}{T_0} [\nabla \cdot T_1(\nabla T_1) - (\nabla T_1)^2]$$

3.99

Applying vector calculus identities to fifth and seventh terms of 3.96, we obtain the following equations.

$$\left(\frac{\vec{B}_0 \cdot \vec{B}_1}{\mu_0}\right) \nabla \cdot \vec{v}_1 = \frac{1}{\mu_0} \{\nabla \cdot [(\vec{B}_0 \cdot \vec{B}_1)\vec{v}_1] - \vec{v}_1 \cdot \nabla(\vec{B}_0 \cdot \vec{B}_1)\}$$

3.100

$$(\vec{B}_0 \cdot \vec{B}_0)(\nabla \cdot \vec{v}_1) = (\vec{B}_0 \times \vec{B}_0) \cdot (\nabla \times \vec{v}_1) + (\vec{B}_0 \cdot \nabla)(\vec{B}_0 \cdot \vec{v}_1)$$

$$(\vec{B}_0 \cdot \vec{B}_0)(\nabla \cdot \vec{v}_1) = (\vec{B}_0 \cdot \nabla)(\vec{B}_0 \cdot \vec{v}_1)$$

3.101

Substituting 3.98, 3.99 and 3.101 into 3.96, the following representation of the RHS of 3.92 is obtained:

$$-\nabla \cdot \left[p_1 \vec{v}_1 - \frac{T_1}{T_0}(\kappa \nabla T_1)\right] + \frac{4}{3}\mu\{\nabla \cdot [\vec{v}_1(\nabla \cdot \vec{v}_1)] - (\nabla \cdot \vec{v}_1)^2\} - \vec{v}_1 \cdot (\vec{B}_0 \times \vec{J}_1) + \rho_1 \vec{v}_1 \cdot \vec{g}$$

$$- \frac{1}{\mu_0}\{\nabla \cdot [(\vec{B}_0 \cdot \vec{B}_1)\vec{v}_1] - \vec{v}_1 \cdot \nabla(\vec{B}_0 \cdot \vec{B}_1)\} - \frac{\kappa}{T_0}(\nabla T_1)^2$$

$$+ \frac{T_1}{\mu_0 T_0}(\vec{B}_0 \cdot \nabla)(\vec{B}_0 \cdot \vec{v}_1)$$

3.102

Grouping terms with divergence in 3.102, we obtain:

$$-\nabla \cdot \left[p_1 \vec{v}_1 - \frac{T_1}{T_0}(\kappa \nabla T_1) - \frac{4}{3}\mu \vec{v}_1(\nabla \cdot \vec{v}_1) + \frac{1}{\mu_0}[(\vec{B}_0 \cdot \vec{B}_1)\vec{v}_1] \right] \qquad \text{3.103a}$$

The other terms (without divergence) in 3.102 are:

$$-\frac{4}{3}\mu(\nabla \cdot \vec{v}_1)^2 - \vec{v}_1 \cdot (\vec{B}_0 \times \vec{J}_1) + \rho_1 \vec{v}_1 \cdot \vec{g} - \frac{\kappa}{T_0}(\nabla T_1)^2 + \frac{1}{\mu_0}\vec{v}_1 \cdot \nabla(\vec{B}_0 \cdot \vec{B}_1) \qquad \text{3.103b}$$

$$+ \frac{T_1}{\mu_0 T_0}(\vec{B}_0 \cdot \nabla)(\vec{B}_0 \cdot \vec{v}_1)$$

Comparing the LHS (3.95) and RHS (3.103a and b) with 3.82 i.e. $\partial_t w + \nabla \cdot \vec{I} = -\text{D}$

$$w = \frac{1}{2}\left(\rho_0 v_1^2 + \frac{p_1^2}{\rho_0 c_0^2} + \frac{\rho_0 T_0 s_1^2}{c_p} \right) + \frac{\rho_1}{\rho_0}\frac{\vec{B}_0 \cdot \vec{B}_1}{\mu_0} \qquad \text{3.104a}$$

$$\vec{I} = p_1 \vec{v}_1 - \frac{T_1}{T_0}(\kappa \nabla T_1) - \frac{4}{3}\mu \vec{v}_1(\nabla \cdot \vec{v}_1) + \frac{1}{\mu_0}[(\vec{B}_0 \cdot \vec{B}_1)\vec{v}_1] \qquad \text{3.104b}$$

$$\text{D} = \frac{4}{3}\mu(\nabla \cdot \vec{v}_1)^2 + \vec{v}_1 \cdot (\vec{B}_0 \times \vec{J}_1) - \rho_1 \vec{v}_1 \cdot \vec{g} + \frac{\kappa}{T_0}(\nabla T_1)^2 - \frac{1}{\mu_0}\vec{v}_1 \cdot \nabla(\vec{B}_0 \cdot \vec{B}_1) \qquad \text{3.104c}$$

$$- \frac{T_1}{\mu_0 T_0}(\vec{B}_0 \cdot \nabla)(\vec{B}_0 \cdot \vec{v}_1) - \frac{\rho_1}{\rho_0}\frac{\vec{B}_0}{\mu_0} \cdot (\partial_t \vec{B}_1)$$

Now that the energy dissipation for corollary for an acoustic wave in a PIP has been derived, the next step is to determine the attenuation coefficient. This is done in the next section.

3.4.4 Determination of Plane Wave Attenuation Coefficient

The classical attenuation coefficient ($\propto_{cl}$) is found using the relation (Pierce, 1981)

$$D_{av} = |D| \approx 2 \propto_{cl} I_{av}, \ \ where \ I_{av} = \frac{\overline{p_1}^2}{\rho_0 c_0} \qquad \text{3.105a}$$

Implicit in the expression for I_{av}, is the assumption that: magnetic pressure is 'insignificant' compared to the acoustic pressure. Since magnetic effects have been added into our

framework, 3.105a can be adapted to finding an expression for magneto-classical attenuation coefficient, $\propto_{cl}^{mag}$ as follows:

$$\propto_{cl}^{mag} \approx \frac{1}{2}\frac{D_{av}}{I_{av}}$$

3.105b

Each term of D (3.104c) is evaluated in the subsequent sections.

3.4.5 Evaluation of the Dissipative (D) Terms

For plane waves, the particle velocity $(\vec{v}_1)$ is obtained as:

$$\vec{v}_1 = \frac{p_1}{\rho_0 c_0}\hat{v}$$

3.106

T_1 is defined in terms of p_1 in equation 3.58. Its gradient is:

$$\nabla T_1 = \left(\frac{\beta_p T_0}{\rho_0 c_p}\right)\nabla p_1 = \left(\frac{\beta_p T_0}{\rho_0 c_p}\right)i\vec{K}p_1 \Rightarrow (\nabla T_1)^2 = -\left(\frac{\beta_p T_0 K}{\rho_0 c_p}\right)^2 (p_1)^2$$

3.107

3.4.5.1 Evaluation of the Term $^4/_3\,\mu(\nabla\cdot\vec{v}_1)^2$

Inserting 3.106 and, $\nabla \equiv i\vec{K}$ where, $\vec{K} = K\hat{k}$ the following representation is obtained:

$$\frac{4}{3}\mu(\nabla\cdot\vec{v}_1)^2 = -\frac{4}{3}\mu\left(\hat{k}\cdot\hat{v}\right)^2\left(\frac{Kp_1}{\rho_0 c_0}\right)^2$$

3.108

3.4.5.2 Evaluation of the term $\vec{v}_1\cdot\left(\vec{B}_0\times\vec{J}_1\right)$

From equation 3.57,

$$\vec{B}_0\times\vec{J}_1 \approx i\tilde{A}_B\rho_0 v_A^2\left\{\left[\left(\vec{K}\cdot\hat{b}_0\right)\left(\hat{b}_0\cdot\vec{v}_1\right) - \left(\vec{K}\cdot\vec{v}_1\right)\right]\vec{K} - \left(\vec{K}\cdot\hat{b}_0\right)^2\vec{v}_1 + \left(\hat{b}_0\cdot\vec{K}\right)\left(\vec{K}\cdot\vec{v}_1\right)\hat{b}_0\right\}$$

3.109

hence,

$$\vec{v}_1 \cdot (\vec{B}_0 \times \vec{J}_1) = i\tilde{A}_B \rho_0 v_A^2 \left\{ \left[(\vec{K} \cdot \hat{b}_0)(\hat{b}_0 \cdot \vec{v}_1) - (\vec{K} \cdot \vec{v}_1) \right](\vec{v}_1 \cdot \vec{K}) - (\vec{K} \cdot \hat{b}_0)^2 (\vec{v}_1 \cdot \vec{v}_1) \right. \tag{3.110}$$

$$\left. + (\hat{b}_0 \cdot \vec{K})(\vec{K} \cdot \vec{v}_1)(\vec{v}_1 \cdot \hat{b}_0) \right\}$$

Inserting 3.106 and $\vec{K} = K\hat{k}$, the following equation is obtained and further simplified.

$$\vec{v}_1 \cdot (\vec{B}_0 \times \vec{J}_1) = i\tilde{A}_B \rho_0 v_A^2 \left\{ \left[(\vec{K} \cdot \hat{b}_0)(\hat{b}_0 \cdot \vec{v}_1)(\vec{v}_1 \cdot \vec{K}) - (\vec{K} \cdot \vec{v}_1)^2 \right] - (\vec{K} \cdot \hat{b}_0)^2 (\vec{v}_1 \cdot \vec{v}_1) \right. \tag{3.111a}$$

$$\left. + (\hat{b}_0 \cdot \vec{K})(\vec{K} \cdot \vec{v}_1)(\vec{v}_1 \cdot \hat{b}_0) \right\}$$

$$= i\tilde{A}_B \rho_0 v_A^2 \left(\frac{Kp_1}{\rho_0 c_0} \right)^2 \left\{ \left[(\hat{k} \cdot \hat{b}_0)(\hat{b}_0 \cdot \hat{v})(\hat{k} \cdot \hat{v}) - (\hat{k} \cdot \hat{v})^2 \right] - (\hat{k} \cdot \hat{b}_0)^2 (\hat{v} \cdot \hat{v}) \right. \tag{3.111b}$$

$$\left. + (\hat{b}_0 \cdot \hat{k})(\hat{k} \cdot \hat{v})(\hat{v} \cdot \hat{b}_0) \right\}$$

$$\vec{v}_1 \cdot (\vec{B}_0 \times \vec{J}_1) = i\tilde{A}_B \rho_0 v_A^2 \left(\frac{Kp_1}{\rho_0 c_0} \right)^2 \left[2(\hat{k} \cdot \hat{b}_0)(\hat{b}_0 \cdot \hat{v})(\hat{k} \cdot \hat{v}) - (\hat{k} \cdot \hat{v})^2 - (\hat{k} \cdot \hat{b}_0)^2 \right] \tag{3.111c}$$

3.4.5.3 Evaluation of the Term $\rho_1 \vec{v}_1 \cdot \vec{g}$

From the linearized mass continuity equation

$$\partial_t \rho_1 = -\rho_0 \nabla \cdot \vec{v}_1$$

$$-i\omega \rho_1 = -i\rho_0 K\hat{k} \cdot \frac{p_1}{\rho_0 c_0} \hat{v}$$

$$\rho_1 = \frac{Kp_1}{\omega c_0} \hat{k} \cdot \hat{v} \tag{3.112}$$

substituting 3.112 into the 3rd term of 104c, the following expression is obtained and further simplified:

$$\rho_1 \vec{v}_1 \cdot \vec{g} = -\frac{Kp_1}{\omega c_0} \hat{k} \cdot \hat{v} \frac{p_1}{\rho_0 c_0} \hat{v} \cdot g\hat{z} = -\frac{g\rho_0}{\omega K} \left(\frac{Kp_1}{\rho_0 c_0} \right)^2 (\hat{k} \cdot \hat{v})(\hat{v} \cdot \hat{z})$$

$$\rho_1 \vec{v}_1 \cdot \vec{g} = -\frac{g\rho_0 c_0}{\omega^2} \left(\frac{Kp_1}{\rho_0 c_0} \right)^2 (\hat{k} \cdot \hat{v})(\hat{v} \cdot \hat{z}) \tag{3.113}$$

3.4.5.4 Evaluation of the Term $\kappa/T_0 \, (\nabla T_1)^2$

Applying 3.107 to the fourth term of 3.104c, the following is obtained:

$$\frac{\kappa}{T_0}(\nabla T_1)^2 = -\frac{\kappa}{T_0}\left(\frac{\beta_p T_0 K}{\rho_0 c_p}\right)^2 (p_1)^2 \tag{3.114}$$

Inserting the following expression for β_p^2 (Pierce, 1981)

$$\beta_p^2 = \frac{(\gamma - 1)c_p}{T_0 c_0^2} \tag{3.115}$$

$$\frac{\kappa}{T_0}(\nabla T_1)^2 = -\frac{\kappa}{T_0}\frac{(\gamma - 1)c_p}{T_0 c_0^2}\left(\frac{T_0 K}{\rho_0 c_p}\right)^2 (p_1)^2 = -\frac{(\gamma - 1)\kappa}{c_p}\left(\frac{K p_1}{\rho_0 c_0}\right)^2 \tag{3.116}$$

3.4.5.5 Evaluation of the Term $1/\mu_0 \, \vec{v}_1 \cdot \nabla(\vec{B}_0 \cdot \vec{B}_1)$

Applying 3.52 i.e. $\vec{B}_1 = \tilde{A}_B(\sigma_e, \omega)\left[(\vec{K} \cdot \vec{B}_0)\vec{v}_1 - (\vec{K} \cdot \vec{v}_1)\vec{B}_0\right]$ to the fifth term of 3.104c:

$$\frac{1}{\mu_0}\vec{v}_1 \cdot \nabla(\vec{B}_0 \cdot \vec{B}_1) = \frac{\tilde{A}_B}{\mu_0}\vec{v}_1 \cdot \nabla\left[(\vec{B}_0 \cdot \vec{v}_1)(\vec{K} \cdot \vec{B}_0) - B_0{}^2(\vec{K} \cdot \vec{v}_1)\right] \tag{3.117}$$

Substituting for $\vec{v}_1, \vec{B}_0, \nabla$ and $\vec{K}$

$$\frac{1}{\mu_0}\vec{v}_1 \cdot \nabla(\vec{B}_0 \cdot \vec{B}_1) = \frac{\tilde{A}_B}{\mu_0}\frac{p_1}{\rho_0 c_0}\hat{v} \cdot iK\hat{k}\left[\left(B_0\hat{b}_0 \cdot \frac{p_1}{\rho_0 c_0}\hat{v}\right)(K\hat{k} \cdot B_0\hat{b}_0) - B_0{}^2\left(K\hat{k} \cdot \frac{p_1}{\rho_0 c_0}\hat{v}\right)\right]$$

$$\frac{1}{\mu_0}\vec{v}_1 \cdot \nabla(\vec{B}_0 \cdot \vec{B}_1) = \frac{i\tilde{A}_B B_0{}^2}{\mu_0}\left[(\hat{b}_0 \cdot \hat{v})(\hat{k} \cdot \hat{b}_0)(\hat{k} \cdot \hat{v}) - (\hat{k} \cdot \hat{v})^2\right]\left(\frac{K p_1}{\rho_0 c_0}\right)^2 \tag{3.118}$$

3.4.5.6 Evaluation of the term $T_1/\mu_0 T_0 \, (\vec{B}_0 \cdot \nabla)(\vec{B}_0 \cdot \vec{v}_1)$

Substituting for $T_1, \vec{B}_0, \nabla$ and $\vec{v}_1$ in the sixth term of 3.104c:

$$\frac{T_1}{\mu_0 T_0}(\vec{B}_0 \cdot \nabla)(\vec{B}_0 \cdot \vec{v}_1) = \frac{1}{\mu_0 T_0}\left(\frac{\beta_p T_0}{\rho_0 c_p}p_1\right)(B_0\hat{b}_0 \cdot iK\hat{k})\left(B_0\hat{b}_0 \cdot \frac{p_1}{\rho_0 c_0}\hat{v}\right)$$

$$= \frac{iK B_0{}^2 \beta_p c_0^2}{\mu_0 c_p c_0 K^2}(\hat{b}_0 \cdot \hat{k})(\hat{b}_0 \cdot \hat{v})\frac{K^2 p_1{}^2}{\rho_0{}^2 c_0^2}$$

$$\beta_p^2 = \frac{(\gamma - 1)c_p}{T_0 c_0^2} \implies \beta_p = \frac{1}{c_0}\sqrt{\frac{(\gamma - 1)c_p}{T_0}}$$

$$\frac{T_1}{\mu_0 T_0}\left(\vec{B}_0 \cdot \nabla\right)\left(\vec{B}_0 \cdot \vec{v}_1\right) = \frac{iB_0{}^2 c_0}{\mu_0 c_p K}\frac{1}{c_0}\sqrt{\frac{(\gamma - 1)c_p}{T_0}}\left(\hat{b}_0 \cdot \hat{k}\right)\left(\hat{b}_0 \cdot \hat{v}\right)\left(\frac{Kp_1}{\rho_0 c_0}\right)^2$$

$$\frac{T_1}{\mu_0 T_0}\left(\vec{B}_0 \cdot \nabla\right)\left(\vec{B}_0 \cdot \vec{v}_1\right) = \frac{iB_0{}^2 c_0}{\mu_0 c_p \omega}\sqrt{\frac{(\gamma - 1)c_p}{T_0}}\left(\hat{b}_0 \cdot \hat{k}\right)\left(\hat{b}_0 \cdot \hat{v}\right)\left(\frac{Kp_1}{\rho_0 c_0}\right)^2 \qquad \text{3.119}$$

3.4.5.7 Evaluation of the Term $(\rho_1/\rho_0\mu_0)\vec{B}_0 \cdot (\partial_t \vec{B}_1)$

Substituting for $\rho_1, \vec{B}_0, \vec{B}_1$ and $\partial_t = -i\omega$ in seventh term of 3.104c:

$$\frac{\rho_1}{\mu_0\rho_0}\vec{B}_0 \cdot \left(\partial_t \vec{B}_1\right) = -\frac{i\omega\tilde{A}_B}{\mu_0\rho_0}\frac{p_1}{c_0^2}\hat{k} \cdot \hat{v}\left[\left(B_0\hat{b}_0 \cdot \frac{p_1}{\rho_0 c_0}\hat{v}\right)\left(K\hat{k} \cdot B_0\hat{b}_0\right) - B_0{}^2\left(K\hat{k} \cdot \frac{p_1}{\rho_0 c_0}\hat{v}\right)\right]$$

$$\frac{\rho_1}{\mu_0\rho_0}\vec{B}_0 \cdot \left(\partial_t \vec{B}_1\right) = -\frac{i\omega\tilde{A}_B B_0^2}{\mu_0 c_0}\left(\hat{k} \cdot \hat{v}\right)\left[\left(\hat{b}_0 \cdot \hat{v}\right)\left(\hat{k} \cdot \hat{b}_0\right) - B_0{}^2\left(\hat{k} \cdot \hat{v}\right)\right]\frac{Kp_1^2}{\rho_0^2 c_0^2}$$

$$\frac{\rho_1}{\mu_0\rho_0}\vec{B}_0 \cdot \left(\partial_t \vec{B}_1\right) = -\frac{i\tilde{A}_B B_0{}^2}{\mu_0}\left[\left(\hat{b}_0 \cdot \hat{v}\right)\left(\hat{k} \cdot \hat{b}_0\right)\left(\hat{k} \cdot \hat{v}\right) - \left(\hat{k} \cdot \hat{v}\right)^2\right]\left(\frac{Kp_1}{\rho_0 c_0}\right)^2 \qquad \text{3.120}$$

Adding all the evaluated terms of D together, one obtains the following expression:

$$D = -\frac{4}{3}\mu\left(\hat{k} \cdot \hat{v}\right)^2 - \frac{(\gamma - 1)\kappa}{c_p}\left(\frac{Kp_1}{\rho_0 c_0}\right)^2 + \frac{g\rho_0 c_0}{\omega^2}\left(\frac{Kp_1}{\rho_0 c_0}\right)^2\left(\hat{k} \cdot \hat{v}\right)\left(\hat{v} \cdot \hat{z}\right)$$

$$+ i\tilde{A}_B\rho_0 v_A^2\left[2\left(\hat{k} \cdot \hat{b}_0\right)\left(\hat{b}_0 \cdot \hat{v}\right)\left(\hat{k} \cdot \hat{v}\right) - \left(\hat{k} \cdot \hat{v}\right)^2 - \left(\hat{k} \cdot \hat{b}_0\right)^2\right]\left(\frac{Kp_1}{\rho_0 c_0}\right)^2 \qquad \text{3.121}$$

$$- \frac{iB_0{}^2 c_0}{\mu_0 c_p \omega}\sqrt{\frac{(\gamma - 1)c_p}{T_0}}\left(\hat{b}_0 \cdot \hat{k}\right)\left(\hat{b}_0 \cdot \hat{v}\right)\left(\frac{Kp_1}{\rho_0 c_0}\right)^2$$

Further simplification of above equation yields the following equation:

$$D = \left\{ -\frac{4}{3}\mu(\hat{k}\cdot\hat{v})^2 - \frac{(\gamma-1)\kappa}{c_p} + \frac{g\rho_0 c_0}{\omega^2}(\hat{k}\cdot\hat{v})(\hat{v}\cdot\hat{z}) \right.$$

$$+ i\tilde{A}_B\rho_0 v_A^2\left[2(\hat{k}\cdot\hat{b}_0)(\hat{b}_0\cdot\hat{v})(\hat{k}\cdot\hat{v}) - (\hat{k}\cdot\hat{v})^2 - (\hat{k}\cdot\hat{b}_0)^2\right]$$

<div align="right">3.122</div>

$$\left. - \frac{iB_0{}^2 c_0}{\mu_0 c_p \omega}\sqrt{\frac{(\gamma-1)c_p}{T_0}}(\hat{b}_0\cdot\hat{k})(\hat{b}_0\cdot\hat{v}) \right\}\left(\frac{Kp_1}{\rho_0 c_0}\right)^2$$

Following Pierce's (1981) 'recipe', D_{av} is time average, $\overline{D}$ found as follows:

$$D_{av} \cong \overline{D_x} + i\overline{D_y} \implies \propto_{cl}^{mag} = \propto_x(\overline{D_x}) + i\propto_y(\overline{D_y})$$

The real part of $\propto_{cl}^{mag}$ represents absorption while the imaginary part represents dispersion.

From equation 3.105b,

$$\propto_{cl}^{mag} \approx \frac{1}{2}\frac{D_{av}}{I_{av}}$$

<div align="right">3.105c</div>

Hence, the attenuation coefficient can be expressed as follows:

$$\propto_{cl}^{mag} = \frac{1}{2}\frac{\omega^2}{\rho_0 c_0{}^3}\left\{\frac{4}{3}\mu(\hat{k}\cdot\hat{v})^2 + \frac{(\gamma-1)\kappa}{c_p} - \frac{g\rho_0 c_0}{\omega^2}(\hat{k}\cdot\hat{v})(\hat{v}\cdot\hat{z})\right.$$

$$- i\tilde{A}_B\rho_0 v_A^2\left[2(\hat{k}\cdot\hat{b}_0)(\hat{b}_0\cdot\hat{v})(\hat{k}\cdot\hat{v}) - (\hat{k}\cdot\hat{v})^2 - (\hat{k}\cdot\hat{b}_0)^2\right]$$

<div align="right">3.123</div>

$$\left. + \frac{iB_0{}^2 c_0}{\mu_0 c_p \omega}\sqrt{\frac{(\gamma-1)c_p}{T_0}}(\hat{b}_0\cdot\hat{k})(\hat{b}_0\cdot\hat{v})\right\}$$

3.4.5.8 The Attenuation Coefficient for Acoustic Waves

The following attenuation coefficient is obtained from 3.123 when acoustic waves propagate along the direction of the magnetic field i.e. $\hat{k}\cdot\hat{v} = 1, \hat{k}\cdot\hat{b}_0 = 1, \hat{b}_0\cdot\hat{v} = 1$ and $\hat{v}\cdot\hat{z} = 1$.

<div align="right">3.125</div>

$$\propto_{cl}^{mag} = \frac{1}{2}\frac{\omega^2}{\rho_0 c_0{}^3}\left[\frac{4\mu}{3} + \frac{(\gamma-1)\kappa}{c_p} - \frac{g\rho_0 c_0}{\omega^2} + \frac{iB_0{}^2 c_0}{\mu_0 c_p \omega}\sqrt{\frac{(\gamma-1)c_p}{T_0}}\right]$$

In the absence of thermo-viscous losses ($\mu = \kappa = 0$) and neglecting gravity ($g = 0$), $\propto_{cl}^{mag}$ is purely imaginary, meaning that it only contributes to wave dispersion. The wave number, expressed as:

$$\widetilde{K}(\omega) = \frac{\omega}{c_0} + i \propto_{cl}^{mag} \qquad \text{3.126a}$$

becomes, in this case:

$$\widetilde{K}(\omega) = \left[\frac{\omega}{c_0} - \frac{1}{2}\frac{\omega B_0{}^2}{\rho_0 c_0^2 \mu_0 c_p}\sqrt{\frac{(\gamma-1)c_p}{T_0}}\right] + i\frac{1}{2}\frac{\omega^2}{\rho_0 c_0{}^3}\left[\frac{4\mu}{3} + \frac{(\gamma-1)\kappa}{c_p} - \frac{g\rho_0 c_0}{\omega^2}\right] \qquad \text{3.126b}$$

$$= \left[\frac{\omega}{c_0} - \frac{1}{2}\frac{\omega v_A^2}{c_0^2 c_p}\sqrt{\frac{(\gamma-1)c_p}{T_0}}\right] + i\frac{1}{2}\frac{\omega^2}{\rho_0 c_0{}^3}\left[\frac{4\mu}{3} + \frac{(\gamma-1)\kappa}{c_p} - \frac{g\rho_0 c_0}{\omega^2}\right]$$

Evaluating the above wave number at 100 km for $f = 0.5\ Hz$ yields the following value:

$$\widetilde{K} = 0.01100913 - i0.00005199, \Longrightarrow c \approx 286\ ms^{-1}\ \&\ \propto\ \approx -0.452\ dB(km)^{-1} \qquad \text{3.127}$$

The wave number 3.127 is then compared to those obtained in the pure acoustic mode via the MHD approach i.e.

$$\widetilde{K}_1 = 0.01110739 + i0.00000952, \Longrightarrow c \approx 283\ ms^{-1}\ \&\ \propto\ \approx 0.083\ dB(km)^{-1}$$

$$\widetilde{K}_2 = 0.01223192 + i14.27466025, \Longrightarrow c \approx 257\ ms^{-1}\ \&\ \propto\ \approx 123{,}990\ dB(km)^{-1}$$

The wave number obtained via EDC approach lends credence to the validity of the $re[\widetilde{K}]$ obtained via MHD. The attenuation coefficient obtained via EDC represents energy gain and is nearly 5 times larger than its MHD counterpart.

3.4.5.9 The Attenuation Coefficient for Magnetosonic Waves

When the acoustic wave propagates perpendicularly to the magnetic field lines ($\hat{k} \cdot \hat{v} = 1$, $\hat{k} \cdot \hat{b}_0 = 0, \hat{b}_0 \cdot \hat{v} = 0$ and $\hat{v} \cdot \hat{z} = 0$). The following attenuation coefficient is obtained:

$$\propto_{cl}^{mag} = \frac{1}{2}\frac{\omega^2}{\rho_0 c_0{}^3}\left\{\frac{4\mu}{3} + \frac{(\gamma - 1)\kappa}{c_p} + i\tilde{A}_B \rho_0 v_A^2\right\} \tag{3.128}$$

$$\Rightarrow \tilde{K}(\omega) = \left[\frac{\omega}{c_0} - \frac{1}{2}\frac{\omega^2 \tilde{A}_B v_A^2}{c_0{}^3}\right] + i\frac{1}{2}\frac{\omega^2}{\rho_0 c_0{}^3}\left[\frac{4\mu}{3} + \frac{(\gamma - 1)\kappa}{c_p}\right] \tag{3.129}$$

Substituting the following expression into 3.129,

$$\tilde{A}_B(\sigma_e, \omega) = \frac{i}{\left(\dfrac{K^2}{C_e} - i\omega\right)}$$

and after some complex number manipulations, the following expression is found:

$$\propto_{cl}^{mag} = \frac{1}{2}\frac{\omega^2}{\rho_0 c_0{}^3}\left[\frac{4\mu}{3} + \frac{(\gamma - 1)\kappa}{c_p} - \frac{\rho_0 v_A^2 K^2 C_e}{K^4 + \omega^2 C_e^2} - i\frac{\omega \rho_0 v_A^2 C_e}{K^4 + \omega^2 C_e^2}\right] \tag{3.130}$$

$$\Rightarrow \tilde{K}(\omega) = \left[\frac{\omega}{c_0} + \frac{1}{2}\frac{\omega^3 v_A^2 C_e}{c_0{}^3(K^4 + \omega^2 C_e^2)}\right] + i\frac{1}{2}\frac{\omega^2}{\rho_0 c_0{}^3}\left[\frac{4\mu}{3} + \frac{(\gamma - 1)\kappa}{c_p} - \frac{\rho_0 v_A^2 K^2 C_e}{K^4 + \omega^2 C_e^2}\right] \tag{3.131}$$

Evaluating the above wave number at 100 km for $f = 0.5\ Hz$ yields the following numbers:

$$\tilde{K}_1 = 0.01110808 + i0.00000952, \tag{3.132a}$$

$$\Rightarrow c \approx 283\ ms^{-1}\ \&\ \propto\ \approx 0.083\ dB(km)^{-1}$$

$$\tilde{K}_2 = 0.00000142 + i0.00000142, \tag{3.132b}$$

$$\Rightarrow c \approx 2{,}259{,}160\ ms^{-1}\ \&\ \propto\ \approx 0.012\ dB(km)^{-1}$$

The first solution agrees with $\tilde{K}_1$ obtained in the MHD approach shown below

$$\tilde{K}_1 = 0.01110806 + i0.00000952, \Rightarrow c \approx 283\ ms^{-1}\ \&\ \propto\ \approx 0.083\ dB(km)^{-1}$$

$$\tilde{K}_2 = 0.01223192 + i14.27466025, \Rightarrow c \approx 257\ ms^{-1}\ \&\ \propto\ \approx 123{,}990\ dB(km)^{-1}$$

$$\tilde{K}_3 = 0.00000079 + i0.00000079, \Rightarrow c \approx 3{,}978{,}300\ ms^{-1}\ \&\ \propto\ \approx 0.007\ dB(km)^{-1}$$

Chapter 4: Conclusions and Recommendations

4.1 Continuum vs. Non-continuum Mechanics

The non-continuum (BU) mechanics approach yielded lower infrasound absorption compared to the continuum (NS) mechanics. This reduction can be attributed to the interdependence of the stress tensor and the heat flux in the non-continuum mechanics. It is expected that, the predicted amplitudes of thermospheric returns produced by the non-continuum approach would show better agreement with measured signals. The decrease in attenuation of acoustic waves produced by the non-continuum approach becomes more pronounced with increasing infrasound frequency. It also increases with altitude, up to about 40% decrease at 160 km. The Burnett treatment results in dispersion, increased sound speed up to about 9% was noted for $f = 0.5\ Hz$ (see Figure 11).

4.2   Electric and Magnetic Effects on Infrasound Dispersion and Attenuation

The two wavenumbers obtained for the pure acoustic mode were also produced by the magnetosonic mode in addition to a third solution of the magnetosonic wave which is likely non-propagating. In the pure acoustic mode, the acoustic wave does no work on the magnetic field i.e. no magnetic field fluctuations are produced. The wave propagates along the magnetic field lines. Hence, the first solution of both the pure acoustic and magnetosonic modes i.e. the wave number with attenuation on the order of 10^{-2} can be regarded as a purely acoustic wave. While, the second solution with attenuation on the order of 10^{5} can be regarded as purely magnetosonic wave. The relatively high attenuation of this magnetosonic wave can be attributed to the work done by the wave on the magnetic field. The magnetosonic wave propagates perpendicularly to the magnetic field lines causing periodic bunching of the magnetic field lines, as shown in Figure 18 below:
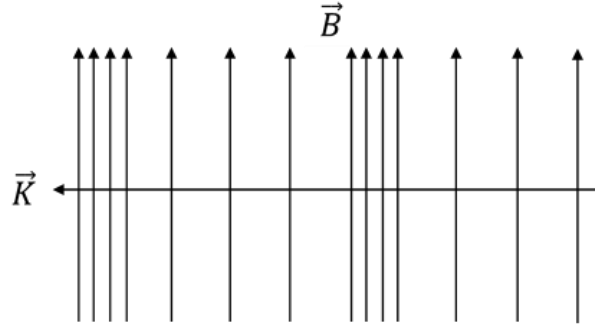
Figure 18: Representation of a magnetosonic wave

4.2.1 Pure Acoustic Wave

In this study, it was observed that the geomagnetic field causes dispersion of acoustic waves (see dependence of $Re[\tilde{K}(\omega)]$ on B_0 in equation 3.98b). How be it 'insignificant' (at $100\ km\ for\ f = 0.5\ Hz$: $281\ ms^{-1}$ without electromagnetic effects compared to $283\ ms^{-1}$ with such effects). Also, the dispersion due to magnetic effects increases with field strength as shown in wave number 3.98b. Dispersion of the magnetosonic wave is also noted as expected (see dependence of $Re[\tilde{K}(\omega)]$ on $v_A\ or\ B_0$ in equation 3.104).

4.3   Recommendations for Future Work

In order to refine and expand the scope of the work done in this study, the following should be considered:

    a) For a neutral thermosphere:

1)   Significant molecular absorption mechanisms due to other air constituents such as O_2, Ar and CO_2 should be considered.

2)   Evaluation of absorption models for a more realistic air mixture i.e. not just $N_2 - O_2$ mixture.

3) Thermospheric winds, i.e. $\vec{v}_0 \neq 0$ should be accounted for in the absorption models since their contributions to the local ambient sound speed can be significant, affecting ray paths. Conversely, thermospheric arrivals can be inverted to *infer* the winds in the lower thermosphere.

4) Consideration of other cooling and heating mechanisms (e.g. radiative cooling, tidal and gravity-wave heating) within the thermosphere.

b) For a charged thermosphere:

1) Application of the MHD approach using the Burnett approximation of the BTE via the associated coupled equations for the stress tensor and heat flux.

2) Extension of the MHD approach to a two-fluid framework, in which neutrals, on one side, and charged species (electrons and ions) on the other side are treated separately. For example, the electro-dynamical coupling of the two categories of particles will be expressed by the full version of the 'two-fluid' Ohm's law (similar to equation 3.38).

3) Refinement of absorption models developed by considering the variation with altitude of the acceleration due to gravity (important for very low frequency waves), $g = g(z)$ and ambient temperature, $T_0 = T_0(z)$.

4) Contribution of molecular relaxation processes to the dispersion and absorption of multi-component partially ionized plasma environment.

5) Implementation of up-to-date values for the ambient concentrations and thermophysical parameters of electrons, ions and neutral, based on current observations and/or general circulation models.

References

Bass, H. E., Bhattacharyya, J., Garcés, M. A., Hedlin, M., Olson, J. V., and Woodward R. L. (**2006**). "Infrasound," *Acoustics Today, 2*(1), pp. 9-17.

Blanc, E., and Ceranna, L. (**2009**). "Infrasound," http://www.ctbto.org/fileadmin/user_upload/pdf/ISS_Publication/Infrasound_11-16.pdf (Last viewed April 12, 2014)

Ceranna, L., Le Pichon, A., Green, D. N., and Mialle, P. (**2009**). "The Buncefield explosion: a benchmark for infrasound analysis across Central Europe," *Geophysical Journal International, 177*, 491-508. doi:10.1111/j.1365-246X.2008.03998.x

Condon, E. U., and Odishaw, H. (**1967**). *Handbook of physics* (Vol. 2). New York: McGraw-Hill.

de Groot-Hedlin, C., Hedlin, M. A., and Walker, K. (**2011**). "Finite difference synthesis of infrasound propagation through a windy, viscous atmosphere: application to a bolide explosion," *Geophysical Journal International*, 1-16. doi:10.1111/j.1365-246X.2010.04925.x

Gabrielson, T. B. (**1998**). "Infrasound," In Crocker, M. J., (Ed.), *Handbook of Acoustics* (pp. 331-336). New York: John Wiley & Sons, Inc.

Gabrielson, T. B. (**2006**). "Refraction of sound in the atmosphere," *Acoustics Today*, pp. 7-16.

Gainville, O., and Blanc-Benon, P. (**2010**). "*Infrasound propagation in realistic atmosphere using nonlinear ray theory,*" Lyon: Congress Francais d'Acoustique.

Gartenhaus, S. (**1964**). *Elements of plasma physics* (Vol. 1). New York: Holt, Rinehart and Winston.

Hedlin, M. A., Walker, K., Drob, D. P., and de Groot-Hedlin, C. D. (**2012**). "Infrasound: Connecting the Solid Earth, Oceans, and Atmosphere," *Annual Review of Earth and Planetary Sciences, 40*, 327-354. doi:10.1146/annurev-earth-042711-105508

Landau, L. D., and Lifshitz, E. M. (**1959**). *Fluid Mechanics* (Vol. 6). Reading, Massachusetts: Addison-Wesley Publishing Company, Inc.

Mason, W. P. (Ed.). (**1965**). *Physical Acoustics: Principles and Methods* (Vol. 2 A). New York: Academic Press Inc.

Negraru, P. T., Golden, P., & Herrin, E. T. (**2010**). "Infrasound Propagation in the 'Zone of Silence'," *Seismological Research Letters, 81*(4), 615-625. doi:10.1785/gssrl.81.4.615

Pierce, A. D. (**1981**). *Acoustics: An Introduction to Its Physical Principles and Applications* (Vol. 1). New York: McGraw-Hill.

Rees, M. H. (**1989**). *Physics and chemistry of the upper atmosphere.* Cambridge: Cambridge University Press.

Riabov, V. V. (**2000**). "Gas Dynamic Equations, Transport Coefficients, and Effects in Nonequilibrium Diatomic Gas Flows," *Journal of Thermophysics and Heat Transfer, 14*(3).

Schunk, R. W., and Nagy, A. F. (**2009**). *Ionospheres: Physics, Plasma Physics, and Chemistry* (Second ed.). New York: Cambridge University Press.

Sutherland, L. C., and Bass, H. E. (**2004**). "Atmospheric absorption in the atmosphere up to 160 km," *Journal of Acoustic Society of America, 115*(3), 1012-1032. doi:10.1121/1.1631937

Sutherland, L. C., and Daigle, G. A. (**1998**). Atmospheric sound propagation. In M. J. Crocker, *Handbook of acosutics* (pp. 305-329). New York: John Wiley and Sons, Inc.

Wang, J. (**1993**). "Electric Conductivity of the Lower Solar Atmosphere," *Astronomical Society of the Pacific Conference Series, 46*, 465-68.

Akintunde, Akinjide Bachelor of Science, Obafemi Awolowo University, January 2008;
    Master of Science, University of Louisiana at Lafayette, Spring 2014
Major: Physics
Title of Thesis: Preliminary Study of Infrasonic Attenuation and Dispersion in the Lower
    Thermosphere Based on Non-continuum Fluid Mechanics: Developing a Predictive
    Model
Thesis Director: Dr. Andi Petculescu
Pages in Thesis: 77; Words in Abstract: 230

ABSTRACT

A framework for predicting thermospheric attenuation and dispersion of infrasound

between 85 and 160 km is presented. The work is part of a pilot study whose goal is to

complement the currently established models of thermospheric propagation, the standard

being the Sutherland-Bass (SB) model J. Acoust. Soc. Am. 115 (3), 1012-1032 (2004). The SB

model overestimates the attenuation noticeably when compared to attenuation of

thermospheric returns measured by receivers. Based on the Navier-Stokes (NS) equation

and its associated momentum and heat fluxes, the SB model treats the higher atmosphere as

a continuum. However, for a given wavelength, the Knudsen number (Kn) increases rapidly

in the thermosphere due to the high mean free path gradient. For $Kn > 0.01$, the continuum

Navier-Stokes equations are no longer accurate. The present work shows how the predicted

wavenumber changes when non-continuum approximations [the Burnett (BU) equations]

are used. The ambient parameters and thermophysical properties are extracted from NIST,

at the partial pressures of the main constituents (N_2 and O_2). The effects of rotational

relaxation, gravity, neutral-charged and charged-charged particle interactions are addressed.

As expected, the BU results obtained converge to NS results in the region where NS is valid

i.e. for $Kn < 0.01$. A significant reduction in attenuation was observed with non-continuum

approach. Also, the effects of electric and magnetic fields on the dispersion and attenuation

were evaluated. This work was funded by NSF-EPSCoR/Louisiana Board of Regents.

Biographical Sketch

Akinjide Akintunde was born in Ibadan, Nigeria. He obtained a Bachelor of Science (with honors) in Physics from the Obafemi Awolowo University (OAU), Ile–Ife, Nigeria in January, 2008. He taught high school physics while serving his country in the National Youth Service Corps from 2008 to 2009. He joined PricewaterhouseCoopers (PwC) Nigeria in October 2009 as an associate in the firm's assurance practice, providing assurance services to clients in manufacturing, information technology and telecommunications industries. He left PwC as a senior associate in 2012 to pursue a Master of Science degree in Physics at the University of Louisiana at Lafayette, which will be awarded in Spring 2014.